

STRATIGRAPHIC AND DIAGENETIC COMPARISONS OF THE MONTEREY
FORMATION, POINT REYES AND MONTEREY AREAS, CALIFORNIA

A Thesis submitted to the faculty of
San Francisco State University
In partial fulfillment of
The requirements for
The Degree

AS

36

2016

GEOL

.K45

Master of Science

In

Geosciences

by

Burcin Kelez

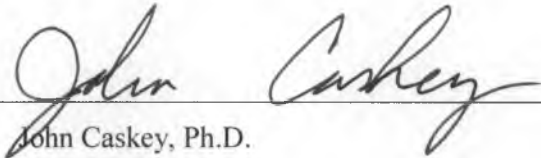
San Francisco, California

May 2016

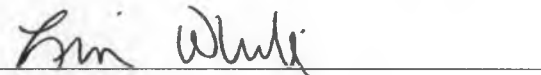
Copyright by
Burcin Kelez
2016

CERTIFICATION OF APPROVAL

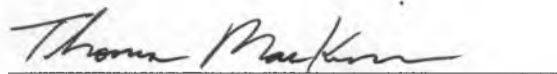
I certify that I have read *Stratigraphic and diagenetic comparisons of the Monterey Formation, Point Reyes and Monterey Areas, California* by Burcin Kelez, and that in my opinion this work meets the criteria for approving a thesis submitted in partial fulfillment of the requirements for the degree: Master of Science in Geosciences at San Francisco State University.



John Caskey, Ph.D.
Associate Professor



Lisa White, Ph.D.
Adjunct Professor



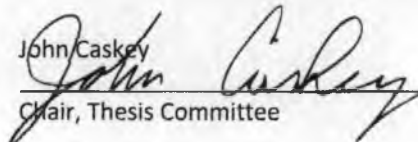
Thomas MacKinnon, Ph.D.
Geologist, retired Chevron

STRATIGRAPHIC AND DIAGENETIC COMPARISONS OF THE MONTEREY FORMATION,
POINT REYES AND MONTEREY AREAS, CALIFORNIA

Burcin Kelez
San Francisco, California
2016

The Miocene Monterey Formation is a deep marine deposit characterized by a high content of biogenic silica and organic matter. The biogenic silica is derived mainly from diatoms. Rock types include diatomaceous rocks and their diagenetic equivalents- chert, porcelanite and siliceous mudstone. The Monterey Formation is the source and reservoir rock for most of the oil and gas resources in California. Although the Monterey Formation in many other places in California is composed of three distinctive members, calcareous, phosphatic, and siliceous, the younger siliceous part is the most extensive facies and is the only member well exposed at Point Reyes and the Monterey area. I have examined the stratigraphic and diagenetic features of the sub-members of the siliceous part of the Monterey Formation at two locations: Pt Reyes and the Monterey area. My methods of study included XRD and petrographic analyses to qualitatively determine the major silica phases of Monterey Formation samples. I drew cross sections at eight localities to calculate the minimum thicknesses of the Monterey sub-members, and constructed three stratigraphic columns. My XRD and petrographic analyses show that the Monterey Formation at Point Reyes is composed of opal-CT cherts, opal-CT porcelanites, and opal-CT and quartz mudstone, and the section is thicker and more siliceous than the Monterey rocks of Monterey area. In the Monterey area, the Monterey Formation is composed of opal-A to opal-CT diatomites, opal-CT porcelanites, and opal-CT and quartz mudstone. For my calculations I used 25°C, 50°C and 55°C geothermal gradients; for Pt Reyes this gave approximately 1138 to 2000 m of minimum burial depth, and 283 to 391 m of erosion; for the Monterey area the results were 1139 to 2000 m of minimum burial, and 259 to 1120 m of overburden pressure. The data suggests that burial and diagenesis at Point Reyes occurred before the overlying Santa Margarita sandstone was deposited as evidenced by an erosional unconformity between Monterey and overlying sandstone. In contrast, in the Monterey area, diagenesis occurred after Santa Margarita sandstone deposition as evidenced by the absence of an erosional unconformity and the lack of enough overburden provided by the entire Monterey section. The Monterey Formation in both locations are not efficient petroleum sources like in southern California in part because of insufficient burial depth.

I certify that the Abstract is a correct representation of the content of this thesis.

John Caskey

Chair, Thesis Committee

May 25, 2016
Date

ACKNOWLEDGEMENTS

Particular thanks are given to my thesis committee: Thomas MacKinnon, John Caskey and Lisa White for their insight, expertise and valuable support during my two-year study. I would like to thank Andrew Ichimura for guiding me to use the X-ray diffraction instrument, and thank Russell McArthur to help me preparing my thin sections, and also acknowledge my graduate peers at San Francisco State University. I would also like to express appreciation to my family and my fiancé for never give up supporting me. Finally, I thank the Turkish Petroleum Corporation for funding this project. This thesis would not been possible without you all.

TABLE OF CONTENTS

LIST OF TABLES	viii
LIST OF FIGURES	ix
LIST OF APPENDICES	xi
1.0. Introduction	1
2.0. Geologic Background	2
2.1. Historical Perspectives on the Monterey Formation.....	2
2.2. Silica Diagenesis in the Monterey Formation.....	7
2.2.1. Rock Types	7
2.2.2. Silica Diagenesis.....	9
2.3. Tectonic History and Structural Features in the Point Reyes and the Monterey Study Areas.....	13
2.3.1. History of Displacement along the San Gregorio and San Andreas Fault Zones	13
2.3.2. General Characteristics of Structures in the Point Reyes and Monterey Areas	15
2.3.2.1. Structural Characteristics in the Point Reyes Area	15
2.3.2.2. Structural Characteristics in the Monterey Area.....	19
3.0. Methods.....	20
3.1. Field Data Collection and Construction of Geologic Cross Sections	20
3.2. Laboratory Procedures	22
3.2.1. Petrographic Analysis	22
3.2.2. X-Ray Diffraction (XRD) Analysis	23

TABLE OF CONTENTS

4.0. Results.....	25
4.1. Stratigraphy of the Point Reyes Structural Block	26
4.1.1. Cross Sections and Stratigraphic Column Constructed	31
4.1.2. Petrographic Analysis of Silica on Monterey Formation	44
4.1.3. X-Ray Mineralogy of Silica on Monterey Formation.....	44
4.2. Diagenetic History of the Monterey Formation at Point Reyes.....	46
4.2.1. Estimated Burial Depths of the Monterey Formation	47
4.3. Stratigraphy of the Monterey Area	51
4.3.1 Cross sections and Stratigraphic Column Constructed.....	56
4.3.2. Petrographic Analysis of Silica on Monterey Formation	65
4.3.3. X-Ray Mineralogy of Silica on Monterey Formation.....	67
4.4. Diagenetic History of the Monterey Formation in the Monterey Area	68
4.4.1. Estimated Burial Depths of the Monterey Formation	70
5.0. Discussion	72
6.0. Conclusion	74
6.1. Stratigraphic Comparison of the Monterey Formation, Point Reyes and Monterey Areas	74
6.2. Diagenetic Comparison of the Monterey Formation, Point Reyes and Monterey Areas	75
6.3 Comparison of the Petroleum Potential of the Monterey Formation between northern and southern California	76
7.0 References.....	77
8.0 Appendices.....	85

LIST OF TABLES

Table	Page
1. Slip history of the SGFZ	15
2. Locations of the rock samples collected, Point Reyes area.....	21
3. Locations of the rock samples collected, Monterey area	22
4. Estimated minimum thicknesses of the lithologic units, Point Reyes area	42
5. XRD results of the Monterey Formation samples, Point Reyes area	46
6. Minimum burial depths of the Monterey Formation members, Point Reyes area ..	51
7. Estimated minimum thicknesses of the lithologic units, Monterey area.....	65
8. XRD results of the Monterey Formation samples, Monterey area.....	68
9. Minimum burial depths of the Monterey Formation members, Monterey area	71

LIST OF FIGURES

Figures	Page
1. Distribution of the Monterey Formation along the California coast.....	3
2. Location of the sedimentary basins in California.....	4
3. Displacement of the correlative Tertiary rock units between Point Reyes and Monterey areas	5
4. Typical sub-units of the Monterey Formation of California	7
5. Silica transformation occurred in the Monterey Formation rocks during diagenesis	8
6. Generalized relations between temperature and rock composition silica transformation	12
7. Simplified geologic map of the Point Reyes area	18
8. Silica mineralogy and XRD signals of silica minerals.....	24
9. Example of XRD signals of silica phases	25
10. Generalized stratigraphy of the Point Reyes area	33
11. Point Reyes geology map showing cross-section locations	34
12. Kehoe Beach cross-section.....	35
13. Siliceous mudstone exposure at Kehoe Beach	36
14. Siliceous mudstone sample collected from Kehoe Beach.....	36
15. Sculptured Beach cross-section.....	37
16. Contorted chert and cherty porcelanite exposure at Sculptured Beach.....	38
17. Chert and porcelanite samples collected from Sculptured Beach	38
18. North of Sculptured Beach cross-section	39

LIST OF FIGURES

19. North of Drakes Bay cross-section.....	40
20. Porcelanite exposure in north of Drakes Bay.....	41
21. Porcelanite samples collected from the north of Drakes Bay	41
22. Stratigraphic column of the sampling locations in the Point Reyes area	43
23. Locations of offshore seismic data near Point Reyes area	49
24. Profile image of WSF-001 seismic line	50
25. Generalized stratigraphy of the Monterey area	55
26. Monterey geology map showing cross-section locations.....	57
27. Northwest of Whispering Pines Park cross-section	58
28. Siliceous mudstone exposure at Whispering Pines Park.....	59
29. Siliceous mudstone sample collected from Whispering Pines Park.....	59
30. Pacific Meadows Park cross-section	60
31. Porcelanite exposure at Pacific Meadows Park.....	61
32. Porcelanite sample collected from the Pacific Meadows Park.....	61
33. Toro Road cross-section	62
34. Diatomite exposure on Toro Road	63
35. Diatomite sample collected from Toro Road	63
36. West of Toro Road cross-section	64
37. Stratigraphic column of the sampling locations in the Monterey area.....	66
38. Stratigraphic and diagenetic comparisons of the Monterey Formation members between Point Reyes and Monterey areas	70

LIST OF APPENDICES

Appendix	Page
A. XRD signals of quartz siliceous mudstone, Point Reyes	85
B. XRD signal of opal-CT siliceous mudstone, Point Reyes.....	86
C. XRD signal of opal-CT porcelanite, Point Reyes	87
D. XRD signal of opal-CT chert, Point Reyes	90
E. XRD signal of dolomite rich porcelanite, Point Reyes	91
F. XRD signal of quartz siliceous mudstone, Monterey area	92
G. XRD signal of opal-CT siliceous mudstone, Monterey area	94
H. XRD signal of opal-CT porcelanite, Monterey area	95
I. XRD signal of opal-CT diatomaceous porcelanite, Monterey area	96
J. XRD signal of opal-A to opal-CT diatomite, Monterey area.....	97
K. XRD signal of detritus diatomite, Monterey area	98

1.0. Introduction

The Miocene Monterey Formation in the California coastal region has drawn the attention of numerous geologic investigations because of its value as a hydrocarbon source rock (Figure 1). The majority of exploration-related studies of the Monterey Formation and overlying reservoir rocks have focused in the Transverse Ranges, the Los Angeles and Ventura Basins, and adjacent offshore areas where the largest associated petroleum concentrations have been identified (MacKinnon, 1989) (Figure 2). The Monterey Formation along the north-central coast of California is much less studied than in the south, although it is known to be a source, and local host rock for a poorly defined petroleum system between Monterey and Point Reyes (MacKinnon, 1989). Throughout much of the Miocene thick diatomaceous and organic-rich sediments accumulated in broad structural basins along the California coast, and most of the siliceous sedimentary rocks formed at this time are included within the Monterey Formation, or Monterey Shale as it is also known as (Figure 1). Numerous studies have focused on the diagenetic transformation of silica phases within the Monterey Formation, in part, because the processes of both silica diagenesis and hydrocarbon maturation are dependent on rock temperature history.

Offshore Miocene basins along the California coast formed concurrently with the development of the San Andreas transform fault system (SAFS). The San Gregorio fault zone (SGFZ) (Figure 3) is an important component of the SAFS and this fault is interpreted to have bisected a large sub-basin of the Monterey Formation that is now separated right-laterally by 150-160 km between the city of Monterey (i.e., the type location for the Monterey Formation) and the Point Reyes region (Clark et al., 1984).

Late Tertiary sedimentary rocks in the Point Reyes region are considered part of the Bodega Basin while those in the Monterey area are part of the Salinas Basin (Figure 2).

Movement along the SGFZ is known to have initiated at about 10 Ma, just following deposition of the Monterey Formation (Clark et al., 1984; Dickinson et al., 2005). Hence, the geologic relations make for an ideal opportunity to compare the stratigraphic and diagenetic characteristics of age-correlative strata of the Monterey Formation that represent eastern and western parts of the same original basin. The major focus of this thesis is therefore, to identify and compare the stratigraphic and diagenetic characteristics of once contiguous strata of Monterey Formation that are now separated by ~150 km between the Point Reyes and the Monterey areas where these strata are exposed. The results of the study provide new information about the diagenetic history of the Monterey Formation and insights regarding a poorly understood Middle Miocene hydrocarbon system that developed along an evolving offshore transform boundary along the north-central California Coast.

2.0. Geologic Background

2.1. Historical Perspectives on the Monterey Formation

By the end of the 19th century many ideas were suggested to explain the origin of the siliceous deposits of the Monterey Formation (Bramlette, 1946). Some geologists suggested that the alteration of volcanic debris and seafloor deposition of silica ooze were the most important factors guiding the formation and characteristics of the Monterey Formation. Fairbanks (1904), and Tolman (1927) were the first geoscientists to determine that the hard siliceous rocks of the Monterey Formation were in part altered diatomaceous sediments but, at that time, it was still believed that the Monterey

Formation had a volcanic source. According to Taliaferro (1933) and Bramlette (1946), the major source of silica in marine environments of the Monterey Formation was thought to be repeated volcanism. Calvert (1966) later demonstrated that highly productive coastal upwelling and great accumulations of diatomaceous sediments were the primary factors in creating the siliceous character of the Monterey Formation, and that volcanism was not required.



Figure 1. Distribution of Miocene Monterey Formation, which is also known as the Monterey Shale, along the California coast.

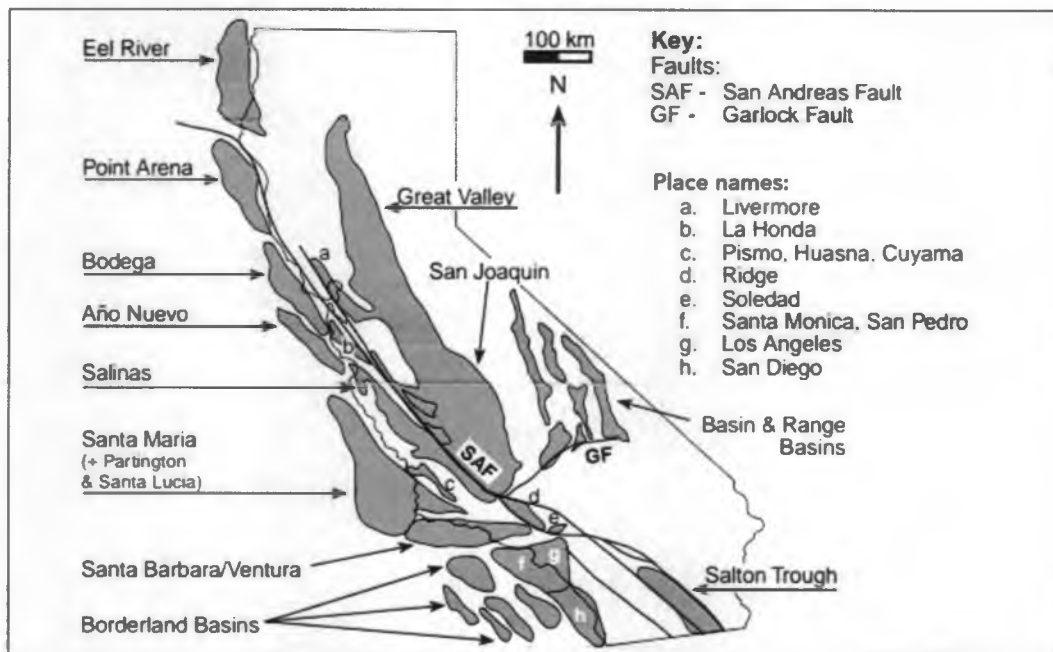


Figure 2. Late Cenozoic sedimentary basins formed along transform faults in California (after Biddle, 1991; and Dunkel and Piper, 1997; in Behl, 1999).

During the 1970s and 1980s, oil exploration along the southern California borderland sparked renewed interest toward understanding the depositional history of the Monterey Formation in offshore basins along the California coast and in the basin-and-ridge topography of the southern California margin (e.g., Ingle et al.;1980; Blake, 1981; Isaacs, 1984; Graham and Williams, 1985; and Lago, 1987). Pisciotto and Garrison (1981) suggested that climatic, oceanographic, and tectonism were all factors in the coastal processes associated with coastal upwelling and ultimately conditions of high plankton productivity recognized previously by Calvert (1966).

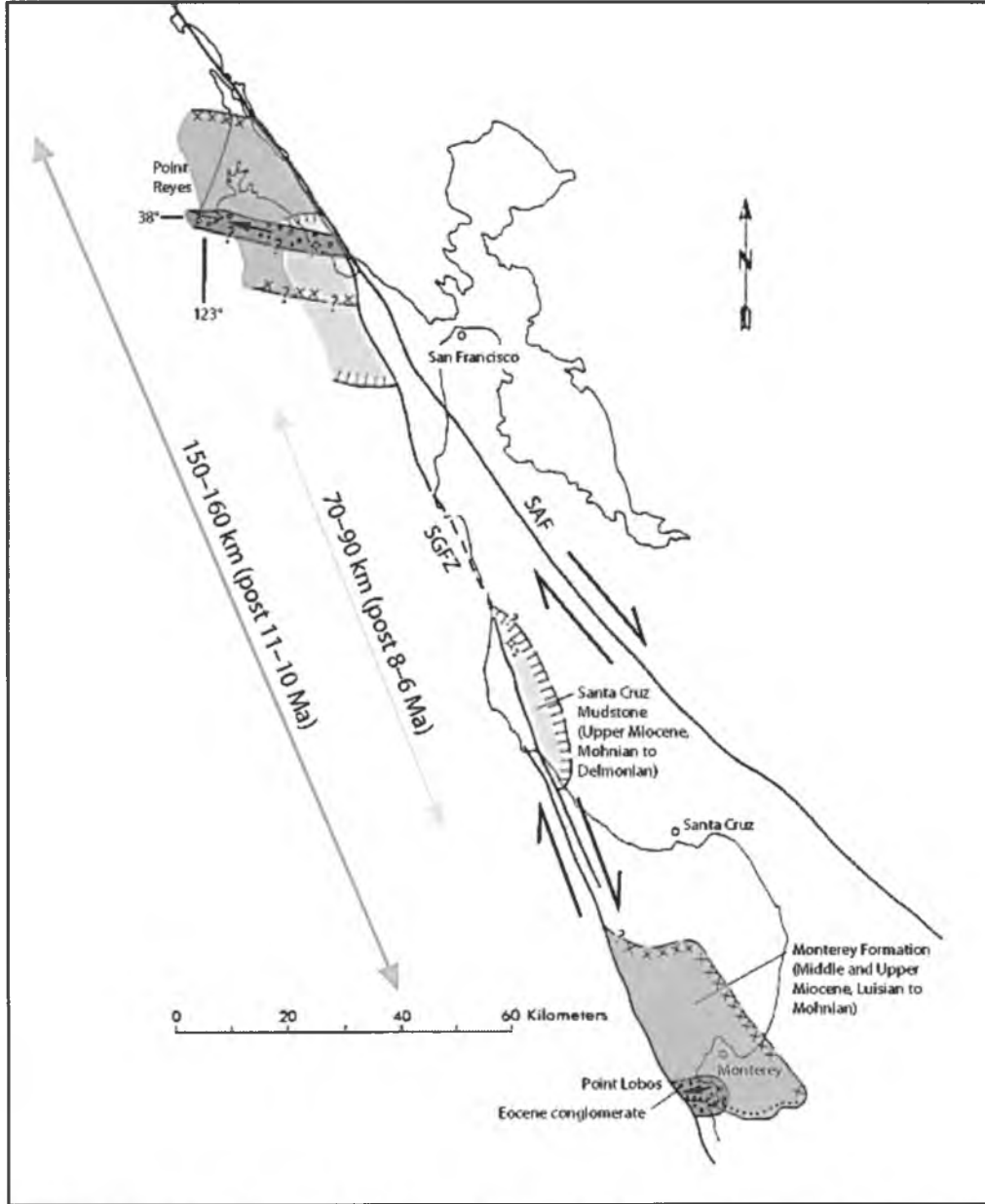


Figure 3. Offset Eocene conglomerate and Miocene basins of the Monterey Formation and Santa Cruz Mudstone between Point Reyes and Monterey (modified from Clark et al., 1984).

Numerous studies have refined the stratigraphy of the Monterey Formation and have revealed that deposits of the Monterey Formation from different basins along the

coast exhibit a remarkably similar pattern of succession of lithofacies, which typically includes; a lower calcareous facies, a middle transitional phosphatic facies, and an upper siliceous facies (e.g., Pisciotto and Garrison, 1981) (Figure 4). However, these studies have also shown that the timing of deposition of the different lithofacies of the Monterey Formation differs between locations along the coast, which suggests that the pattern of facies changes is controlled by factors local to the process of basin development (White, 1989). These relationships have led workers to develop alternative dynamic basin models, whereby organic-rich pelagic and hemi-pelagic deposition of the Monterey Formation is a consequence of local water depths, which are controlled by local subsidence mechanisms that also control the extent and geometry of individual basins that have developed along the coast. The Monterey Formation is now well known to be made up of largely diatomaceous sedimentary rocks. The primary rock types of the formation such as diatomite and diatomaceous mudstone can be difficult to distinguish in the Monterey Formation because they are typically diagenetically altered to porcelanite, chert, siliceous shale, and dolomite (or dolostone) (Isaacs, 1981; Behl, 1992) (Figure 5) The age of the Monterey Formation ranges broadly along the California margin from 17.5 Ma to 6 Ma (Early to Late Miocene). According to MacKinnon (1989), the lower calcareous facies can range in age from 17.5 to 13 Ma, the middle transitional phosphatic facies is typically between 15 Ma and 12 Ma, and the upper siliceous facies can be as young as 5.5 Ma. Diatomaceous deposits accumulated along the California coast until just after 6 Ma, at which time deposition along the California coast experienced “a sudden influx of terrigenous material” (MacKinnon, 1989).

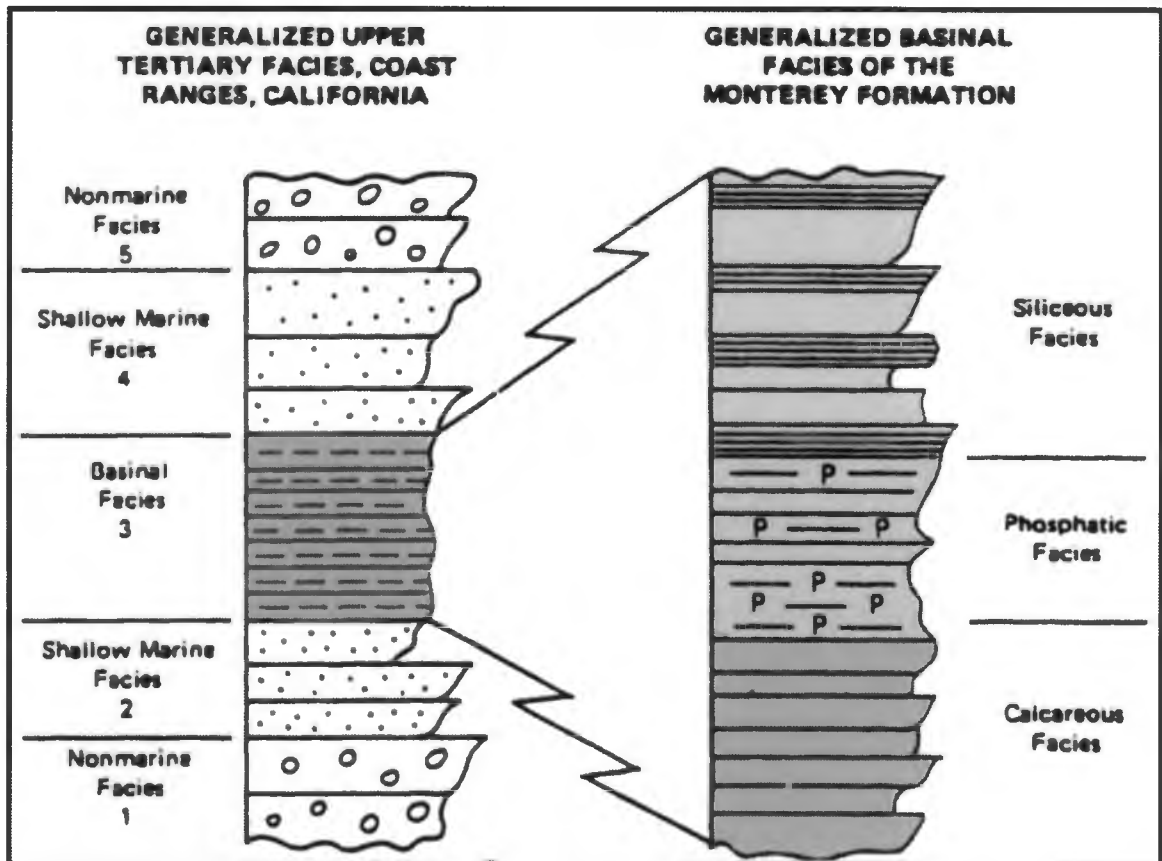


Figure 4. Typical succession of upper Tertiary lithofacies observed along the California coast (left). Basinal deposits of the Monterey Formation generally follow a succession of deposition that includes lower calcareous, middle phosphatic, and upper siliceous facies [from Pisciotto and Garrison (1981) in Behl (1992)].

2.2. Silica Diagenesis in the Monterey Formation

2.2.1. Rock Types

MacKinnon (1989) briefly summarized the siliceous rock types forming the different members of the Monterey Formation along the California coast.

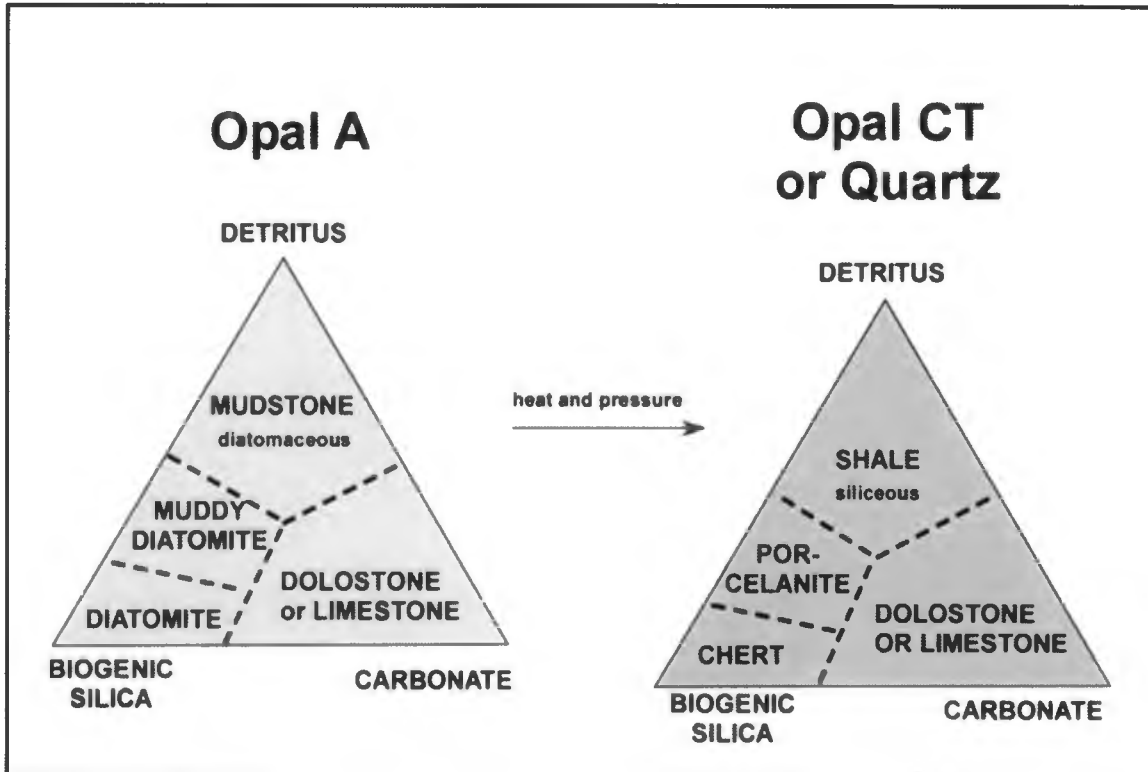


Figure 5. Silica transformation during diagenesis in Monterey Formation rocks (modified from MacKinnon, unpublished data). This simplistic diagram does not include the effects of silica or carbonate migration, which can be substantial in some situations.

Diatomaceous rock is laminated, very porous, lightweight and soft, buff-white to brownish in weathered outcrops and darker where fresh. Diatomite powders when it is scratched or it can show a waxy texture if it has a high diatom content. Siliceous mudstone or siliceous shale is a fine-grained and may be massive or laminated. When it is scratched, it has a waxy look. Porcelanite is similar to unglazed porcelain. It is very fine grained, typically laminated, white to brownish colored, and can be scratched with a knife since its hardness is less than 5. Chert is also very fine-grained, white to brown to black in color, and usually has a glassy texture. In contrast to porcelanite, its hardness is greater

than 5 and a knife cannot scratch it. Marl is similar in appearance to siliceous mudstone. It is white to yellowish in color, and reacts with dilute Hydrogen Chloride (HCL). Dolostone also fizzes in dilute HCL if scratched first. This fine-to-medium grained, massive rock can be scratched easily even though it is a resistant rock in outcrop. Its color varies from gray, yellow to brown.

2.2.2. Silica Transformation

The primary silica in the Monterey Formation is mainly from diatom shells, radiolarian, and other silica-based microorganisms, and predominantly consists of opal-A silica ($\text{SiO}_2 \cdot n\text{H}_2\text{O}$), which is a hydrous, amorphous, and unstable silica phase. With burial, an increase in rock temperature will cause the primary opal-A silica to diagenetically transform to a more stable and ordered form of silica, opal-CT (SiO_2), which corresponds to the minerals Crystobalite and Tridymite. With further burial, temperatures can increase to levels where opal-CT will transform to microcrystalline quartz, the most stable phase of silica.

The transformation of silica to more stable and ordered phases is accompanied by considerable decreases in the porosity, increases in the density of the silica-bearing rocks, and significant changes in the rock's pore water chemistry. With the transformation from opal-A to opal-CT, soft, punky, low-density diatomite and diatomaceous mudstone will diagenetically alter to hard and brittle rocks such as siliceous mudstone, porcelanite, and chert, which are much denser and less porous than the original rock types. Further decrease in porosity and increase in density accompanies the diagenesis of opal-CT to quartz, although this transformation does not usually result in further recognizable changes in the appearance of the silica-bearing rocks.

A significant body of research on the process of silica diagenesis (Keller and Isaacs, 1985) has resulted in a well-accepted, general understanding of the relationship between temperatures required for silica diagenesis and the relative concentrations of silica versus detritus content in the original sediment. According to Keller and Isaacs (1985), temperature is the major factor controlling the diagenetic process (Figure 6). The required temperature range to transform opal-A to opal-CT is from approximately 42° to 48° C (108° to 118° F), and opal-CT to quartz is from approximately 62° to 82° C (144° to 180° F) for siliceous mudstone and porcelanite.

Rock composition is also an important factor in mineral conversion during diagenesis. Rocks with a high biogenic silica to detritus ratio convert from opal A to CT at lower temperatures and from CT to quartz at higher temperatures compared to rocks with lower biogenic to detritus ratios (Isaacs, 1982) as shown in figure 6. Note that detrital quartz is included in the detritus category and must be distinguished from biogenic (authigenic) quartz in these calculations.

According to Leinen (1977), the abundance of detrital (non-biogenic) silica can be calculated using the empirical formula of, $4.33A + 1.35Mg^2$. When the result is subtracted from the total silica content, it gives us the content of the biogenic+diagenetic silica in the sample. Littke et al. (1991) indicates that the carbonate content is not critical for opal transformation unless it is more than 85%.

In terms of rock types, compositional control of diagenesis (Figure 6), results in opal-CT cherts forming earlier than opal-CT porcelanite, and most quartz cherts forming before the opal-CT to quartz transformation in mudstones and porcelanites (Behl, 1992). On the other hand, there are instances where diatomites and rare opal-CT chert spheroids can be present at the same temperature range; this occurs by dissolution of silica in diatomites and precipitation nearby in the form of chert spheroids.

MacKinnon (1989) emphasizes that the burial depth, required for transforming opal-A to opal-CT and opal-CT to quartz is controlled by burial depth and heat flow and these factors vary in different basins along the California coast. MacKinnon (1989) states that the range of the today's geothermal gradient is from $\sim 25^{\circ}$ to 50° C/km in the Monterey basins along the California coast, and it corresponds to depths of ~ 600 to 1400 m to convert opal-A to opal-CT, and of ~ 1200 to 2800 m to convert opal-CT to quartz (assuming a surface temperature as 15° C). Keller and Isaacs (1985) estimate the range of stratigraphic thicknesses of the transition zone for complete transformation of opal-A to opal-CT, and of opal-CT to quartz, which is from 20 to 300 m.

Behl (1992) indicates that the processes and timing of chertification is important to understand other aspects of the diagenetic history of the Monterey Formation. He suggests that much of deformation observed in the Monterey Formation such as contorted beds and other evidence of downslope movements resulted from the volumetric changes (i.e., rock densification and porosity loss) associated with silica diagenesis. Chert in the Monterey Formation exhibits many other abundant and diverse features including sand dikes, chert spheroids, intensive jointing and brecciation that all provide clues to the timing, rates, and other aspects of the chertification process.

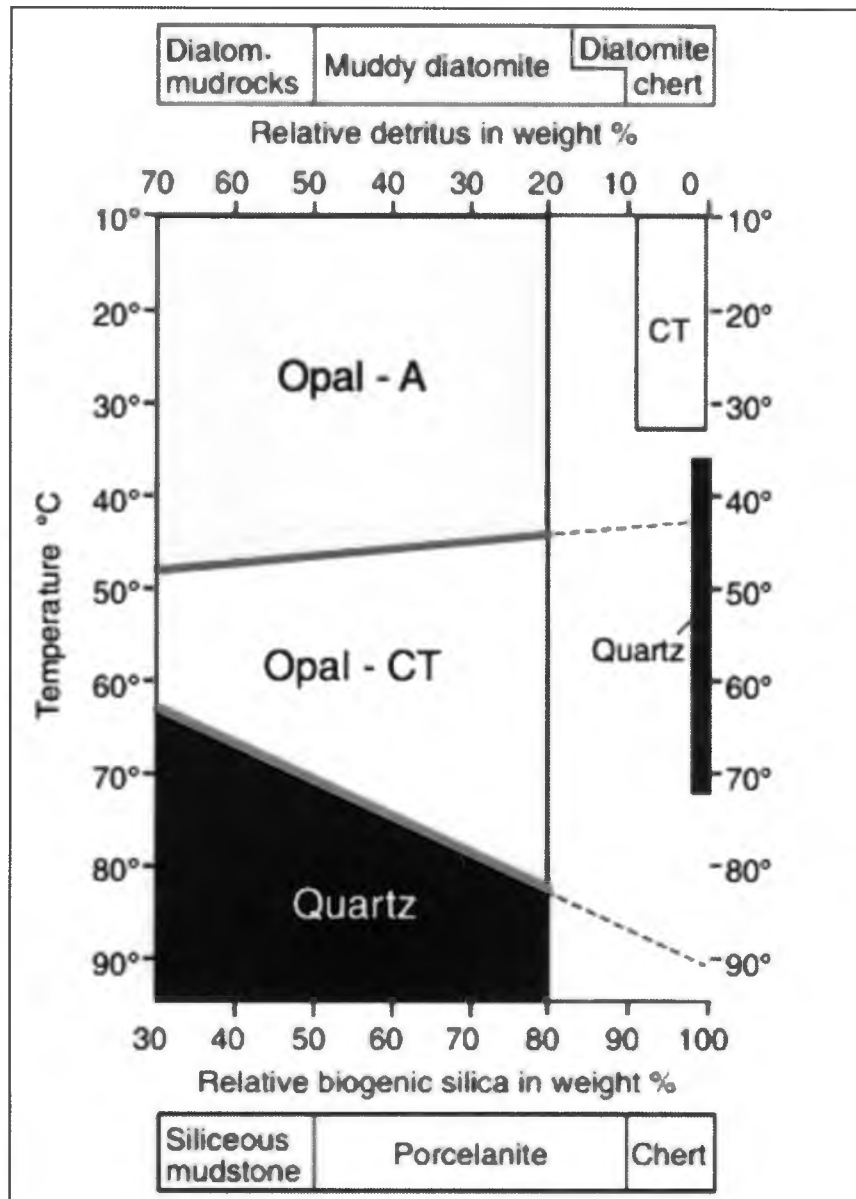


Figure 6. Diagram showing generalized relations between temperature and rock composition during silica transformation through diagenesis (modified from Keller and Isaacs, 1985).

2.3. Tectonic History and Structural Features in the Point Reyes and the Monterey Study Areas

2.3.1. History of Displacement along the San Gregorio and San Andreas Fault Zones

Deposition of the Monterey Formation occurred contemporaneously with the development of the offshore San Andreas (transform) fault system.

The transition along the western North American margin from subduction of the Farallon plate to the transform boundary between the Pacific and North American plates was initiated ~29 m.y. ago at the latitude of the south central California coast (Atwater, 1970). It has since developed and grown to its present-day length of ~1300 km extending northwest from the Gulf of California on the south to Cape Mendocino on the north. The transform system along the central California coast has a complex history of development that involves the broad distribution of distributed shear across an ever-evolving system of multiple active fault strands, large-scale, clockwise transrotation of the Western Transverse Ranges (Hornafius, 1985; Nicholson et al., 1994), variations the rates of relative plate motion (Atwater and Stock, 1998), and at least one significant change in the direction of relative plate motions at 8-6 Ma (Atwater and Stock, 1998). These processes resulted in a fundamental change in the tectonic regime along the CA coast from transtensional to transpressional.

The principal strands of the SAFS along the north-central coast and Coast Ranges are northwest-striking San Andreas Fault zone (SAFZ) and the north-northwest-striking SGFZ (Figure 3). Right-lateral offsets along the SGFZ and SAFZ together total more than 465 km (e.g., Dickinson et al., 2005), with the SAFZ accounting for 315 km of that displacement. This is well documented from correlation of identical 23-Ma volcanic

rocks found on opposite sides of the fault in the Neenach and Pinnacles areas (Matthews, 1976).

The SGFZ lies mostly offshore, extending on land along only five relatively short sections of the fault including two 20-km-long sections of the coast north of San Simeon, and along the Big Sur coast. There is an 18-km-long coastal section from Point Año Nuevo to San Gregorio Beach, a short (<5 km-long) section of the fault north of Half Moon Bay (i.e., the Seal Cove fault), and finally from Bolinas north to where it merges with the SAFZ along the east side of the Point Reyes structural block.

The slip history of the SGFZ is also well documented (e.g., Dickinson et al., 2005; Clark, 1998). Dickinson et al. (2005) conclude that net dextral offset on the SGFZ is 156 ± 4 km based on the correlation of the Nacimiento Fault which bounds the westernmost margin of the Salinian block. This fundamental fault boundary is truncated along the east side of the SGFZ, along the Big Sur coast and along the west side of the fault in the offshore area near Half Moon Bay. Using correlations of late Cenozoic marine stratigraphic sections, Clark et al. (1984) and Clark (1998) have worked out a detailed history of offset for the SGFZ (Figure 3; Table 1). They determined that 11-10 Ma basin deposits of the Monterey Formation are offset right-laterally 150-160 km between Monterey Bay and the Point Reyes Peninsula. They also correlate Late Miocene deposits of the Santa Cruz Mudstone at Point Reyes to their type locality in the Santa Cruz Mountains indicating about 100 km of offset on the SGFZ since about 8 Ma (Table 1). These slip estimates indicate that amount of offset of the 11-10 Ma Monterey Formation is indistinguishable from the net offset of the Nacimiento Fault on the fault (156 ± 4 km). More importantly, these estimates show that slip on the SGFZ did not initiate until after about 10 Ma (Clark et al., 1984; Clark, 1998) after deposition of the Monterey Formation along the north-central coast.

Table 1. Post-Middle Miocene displacement history for the SGFZ.

early-Late-Miocene (10-8 Ma)	Late-Miocene to early-Pliocene (8-3 Ma)	post-middle-Pliocene (3-0 Ma)	post-late-Pleistocene (post-83 ka)
50-60 km	81 km	19 km	250-350 m
25-30 mm/year	16 mm/year	6 mm/year	3-4 mm/year

Estimated offsets (second row), and average slip rates (third row) correspond to the time intervals shown above in the first row. Miocene and post-Pliocene offset and slip rate estimates are from Clark (1998). The post-late Pleistocene offset and slip rate is from J. Caskey (SFSU, unpublished data).

2.3.2. General Characteristics of Structures in the Point Reyes and Monterey Areas

Detailed examination of the structural geology of the Point Reyes and Monterey areas was not within the scope of this study. However, the analysis of diagenetic aspects of the Monterey Formation required obtaining the best possible constraints on stratigraphic thicknesses of the formation in both study areas. This was accomplished, in part, by the construction of geologic cross sections through parts of both study areas. Although cross section profiles were chosen to avoid areas of major faulting, they inevitably transect areas where strata are folded and offset by minor faults. The purpose of the following section is therefore to describe the general characteristics of structures as expressed on previously published maps for the two areas.

2.3.2.1. Structural Characteristics in the Point Reyes Area

The Point Reyes structural block is bound to the east by the SAFZ along and north of the convergence between the SAFZ and SGFZ, which join to become a single broad zone of faulting that is the SAFZ. Along the entire northeastern side of the Point

Reyes block, the SAFZ exhibits profound geomorphic expression as a northwest-trending linear trough from Bolinas Lagoon, along the length of Olema Valley and northward through the drowned linear valley that is Tomales Bay (Figure 7). The SAFZ juxtaposes Mesozoic Franciscan bedrock on the east against Mesozoic Salinian granitic and minor metamorphic basement rocks on the west, which are in turn overlain by Eocene to Pliocene marine strata.

The predominant structure of the Point Reyes block is the broad, gentle, north-trending Point Reyes syncline. This fold involves all Tertiary units in the area. The west limb of the syncline is largely an expression of hanging wall uplift on the Point Reyes (reverse) fault (Stozek, 2012). The eastern limb appears to reflect due to a persistent vertical component of slip along the Western Boundary fault (Galloway, 1977) which marks the southwesternmost limit of the broader SAFZ. The axis of the syncline is poorly defined but generally extends through the area of very low relief at Drakes Estero which lies centrally between uplifted areas to the west and east.

The Monterey Formation exhibits intensive folding at Sculptured Beach where the Santa Margarita Formation overlies the highly deformed layering of the Monterey Formation along a well exposed angular unconformity. The Monterey Formation strata below the angular unconformity are complexly folded and exhibit intensive layer-parallel shear. Cut-off angles of 70°-90° occur in strata of the Monterey Formation below the unconformity which is marked by the basal conglomerate of the Santa Margarita Sandstone. The intensive folding expressed in the Sculptured Beach area has been interpreted to be tied to diagenesis in the Monterey Formation and therefore the cross-cutting relations in this area provide information regarding the burial and thermal history of the Monterey Formation in the Point Reyes area. This is discussed further in the Results section of this report.

Folds are also present in the Kehoe Beach area. The folds are open-to-gentle, east-west-trending, and involve both the Laird Sandstone and Monterey Formation. The modest amount of north-south shortening associated with the folds is consistent with the presence of two east-west striking reverse faults in the same area. Both faults exhibit north-side up displacement of Salinian basement rocks and likely formed during the same localized episode of north-south shortening as the folds.

Other faults exposed in the Point Reyes area are small, and of small displacement, and they are not shown in the geologic map of Galloway (1977), and Clark et al. (1997).

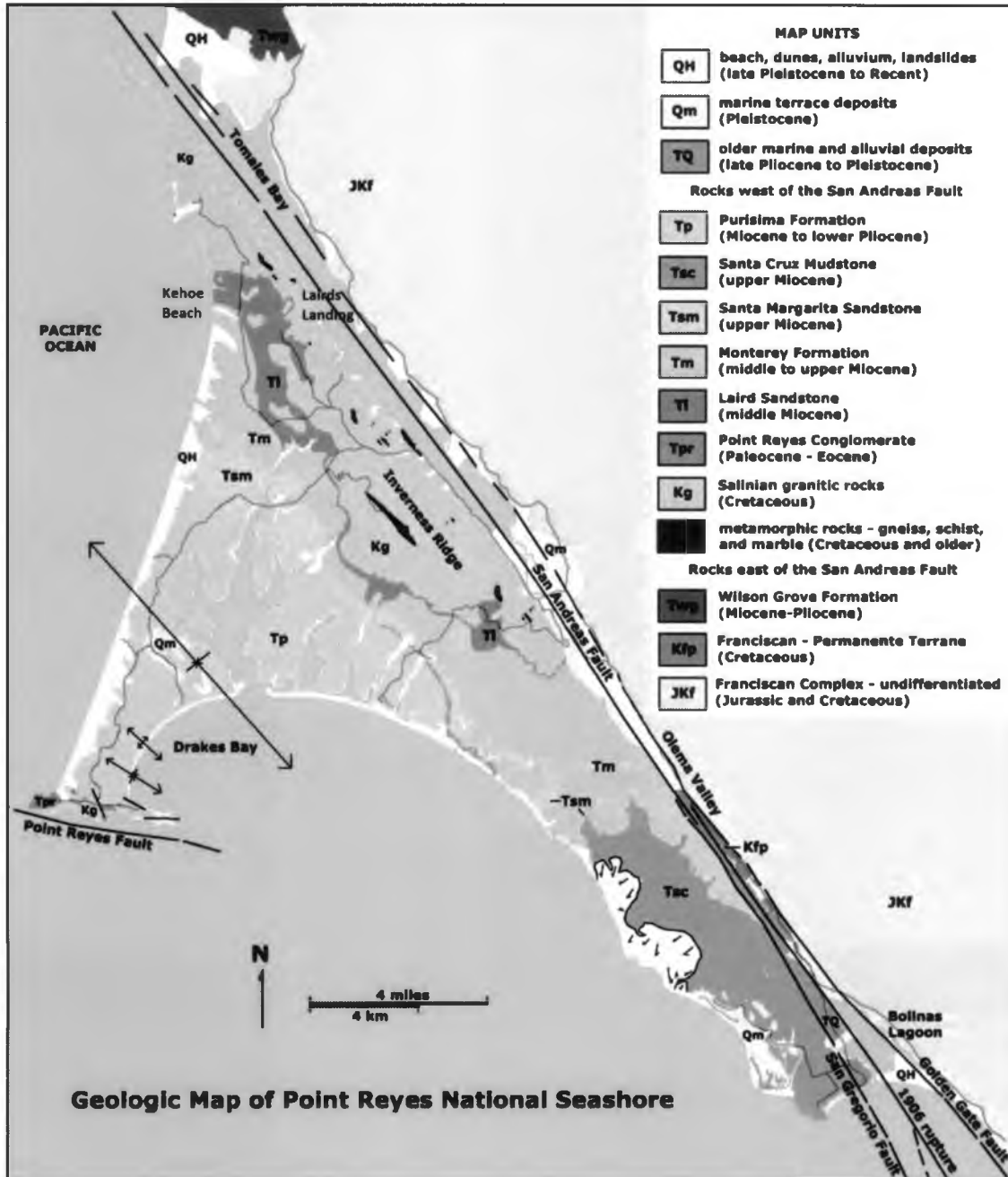


Figure 7. Simplified geologic map of the Point Reyes structural block (after Clark and Brabb, 1997).

2.3.2.2. Structural Characteristics in the Monterey Area

The basement rock throughout the Monterey study area, as in the Point Reyes area is composed of Salinian granitic rocks. The granitic basement together with overlying Monterey Formation and older Tertiary sedimentary rocks are abruptly truncated along the SGFZ which lies only 3 km offshore from Point Lobos (Figure 26).

Numerous fault traces and folds that trend variably from northwest- to west-northwest and even to east-west are expressed in both onshore and offshore parts of the region (Clark et al. 1997; Greene et al., 1990; U.S. Geological Survey digital fault data base) (Figure 26). The northwest-striking faults that project through the area are expressed as discontinuous and distributed. Previous workers have proposed that these faults may collectively account for up to 16 km of right-lateral offset of the Monterey Formation and older rocks in the area (e.g., Graham, 1976; Rosenberg and Clark, 1994). Conversely, other workers (e.g., Dickinson et al., 2004) suggest that large cumulative offsets are not required by the apparent stratigraphic juxtapositions proposed by others. Dickinson et al. (2005) suggest that some right-lateral offset has likely occurred on fault strands that extend northward through the area and into Monterey Bay (e.g., Greene, 1990). Although two cross section profile lines used the Monterey area (see Section 4.3.1) are crossed by faults, the stratigraphic relations used to constrain member thicknesses were not affected by the fault displacements.

3.0. Methods

3.1. Field Data Collection and Construction of Geologic Cross Sections

Field work in the study areas included examining the stratigraphic details and other field relations in key areas of Monterey Formation exposures. Representative rock samples were collected from different members of the Monterey Formation in the Point Reyes and Monterey areas for XRD and petrographic analyses. I also measured stratigraphic sections at three sites for the purpose of determining maximum exposed thicknesses of Monterey Formation members. These sites include: 1) an exposed section of lower siliceous mudstone at Kehoe Beach in the Point Reyes area (Figure 13); 2) a site at Pacific Meadows Park and along Saddle Road (Figure 31) in the Monterey area where the most complete and continuous section of the middle porcelanite member is well exposed; and 3) a section of the upper diatomite member exposed on Toro Road in the Monterey area (Figure 34). Samples for XRD and petrographic analyses were collected along each of the three measured traverses and these include: samples 8.1.T, 8.1.T.1, 8.1.T.2, and 8.6 (Kehoe Beach section, Table 2); samples 6.1 and 15.4 (Pacific Meadows Park and Saddle road section, Table 3); and samples 16.2 and 1.1 (Toro Road section, Table 3). Lab analyses of these samples allowed diagenetic characteristics to be assigned to somewhat specific stratigraphic levels within Monterey Formation members. Locations of all field samples and cross section lines were recorded in the field using hand-held GPS data generated by the smart phone application “Topo Maps.” Sample numbers and locations are summarized in Tables 2 and 3.

Eight cross-sections were constructed to help constrain stratigraphic thicknesses of Monterey Formation members in the Point Reyes and Monterey study areas. Four cross sections for each study area were constructed using structural and stratigraphic data

recorded on published geologic maps (Clark and Brabb, 1997; Clark et al., 1997) in Figures 7 and 26. After studying the structural relations expressed on published maps and in some cases conducting field reconnaissance in the areas of prospective cross section sites (Figure 7 and 26), cross section lines were chosen based on where the most complete exposed stratigraphic sections were most likely to be captured in profile.

Table 2. Locations of the rock samples collected in the Point Reyes area.

Sample ID	Latitude	Longitude	Location name	Monterey member
8.1.T	38.15548 N	122.94850 W	Kehoe Beach	mudstone
8.1.T.1	38.15604 N	122.94742 W	Kehoe Beach	mudstone
8.1.T.2	38.15614 N	122.94951 W	Kehoe Beach	mudstone
8.6	38.15274 N	122.94114 W	Kehoe Beach	mudstone
9.5	38.10087 N	122.90590 W	NW. of Drakes Estero	porcelanite
7.1	38.08881 N	122.93011 W	Oyster Farm	porcelanite
6.1	38.08887 N	122.93037 W	Oyster Farm	porcelanite
3.1	38.09130 N	122.92542 W	N. of Drakes Estero	porcelanite
9.4	38.04948 N	122.85750 W	N. of Sculptured Beach	chert
9.1	38.01253 N	122.85956 W	Sculptured Beach	cherty porcelanite
9.2	38.01100 N	122.84634 W	Sculptured Beach	porcelanite
9.3	38.01080 N	122.84620 W	Sculptured Beach	chert

Table 3. Locations of the rock samples collected in the Monterey area.

Sample ID	Latitude	Longitude	Location name	Monterey member
8.5	36.56994 N	121.92268 W	W of Carmel Woods	mudstone
8.12	36.56702 N	121.92502 W	SW of Carmel Woods	mudstone
9.1	36.57270 N	121.91770 W	SW of Whispering Pines	mudstone
11.1	36.58876 N	121.90079 W	Whispering Pines Park	mudstone
11.5	36.58990 N	121.90301 W	Whispering Pines Park	mudstone
6.1	36.54314 N	121.88377 W	Pacific Meadows Park	porcelanite
15.4	36.54869 N	121.75829 W	Saddle Road	porcelanite
3.2	36.54184 N	121.75200 W	Laureles Grade	diatomaceous
4.1	36.53933 N	121.75101 W	Laureles Grade	diatomaceous
16.2	36.55588 N	121.75178 W	Toro Road	diatomite
1.1	36.55559 N	121.75117 W	Toro Road	diatomite

3.2. Laboratory Procedures

3.2.1. Petrographic Analysis

Thin sections were made from representative specimens for each sample site (Tables 2 and 3). The thin sections were examined under petrographic microscopes and this provided for a qualitative assessment of characteristics such as the dominant silica phases, microfossils, and detritus content that might be expressed in each of the rock specimens sampled from the Monterey and Point Reyes areas. Microscope observations were made in transmitted polarized light. To make the thin sections, I first cut the rock

samples into rectangular slabs to the size of or slightly smaller than the size of a standard glass slide. After finely polishing one side of the rock slabs, I epoxied the polished side of the rock slabs to a pre-frosted glass slide. Finally, I again polished each rock slice until the minerals clearly appear under polarizing light microscope. I prepared 10 thin sections, six of them are from the Point Reyes area, and four of them are from the Monterey area. Diatomite sampled along Toro Road in the Monterey area (Sample 1.1, Table 3) was too soft and porous for thin sectioning. For this sample, a grain mount was prepared for viewing under the microscope.

3.2.2. X-Ray Diffraction (XRD) Analysis

I used a Bruker D8 ADVANCE XRD to determine major biogenic silica phases and the detritus content for each Monterey Formation member in the Point Reyes and Monterey areas. X-ray analysis is necessary to characterize the dominant silica phases and detrital content in a given rock, which in turn informs our understanding of the thermal histories related directly to minimum burial depth for the Monterey Formation strata in the two study areas. To determine which silica phases are present in my samples (e.g., opal-A, opal-CT, and quartz) I analyzed the integrated intensities of key peaks of the diffraction patterns of twenty-three powdered samples (ground to $< 45 \mu\text{m}$). I then compared their diffraction pattern with diffraction patterns of the samples in previous studies to qualitatively identify the presence of the various component phases. I used the quartz crystallinity index (QCI) method of Murata and Norman (1976) to obtain a semi-qualitative estimate of authigenic and detrital quartz in each sample (Figures 8 and 9). Biogenic quartz, a recrystallization product from poorly ordered opaline phases, reveals a single broad peak; whereas, the diffraction pattern of detrital quartz, which is highly ordered and of igneous and metamorphic origin, shows sharp peaks with a distinctive

scattering angle (2θ) between 67° and 69° . Most of my samples contain a mixture of biogenic and detrital quartz and both patterns can be seen in most of my samples.

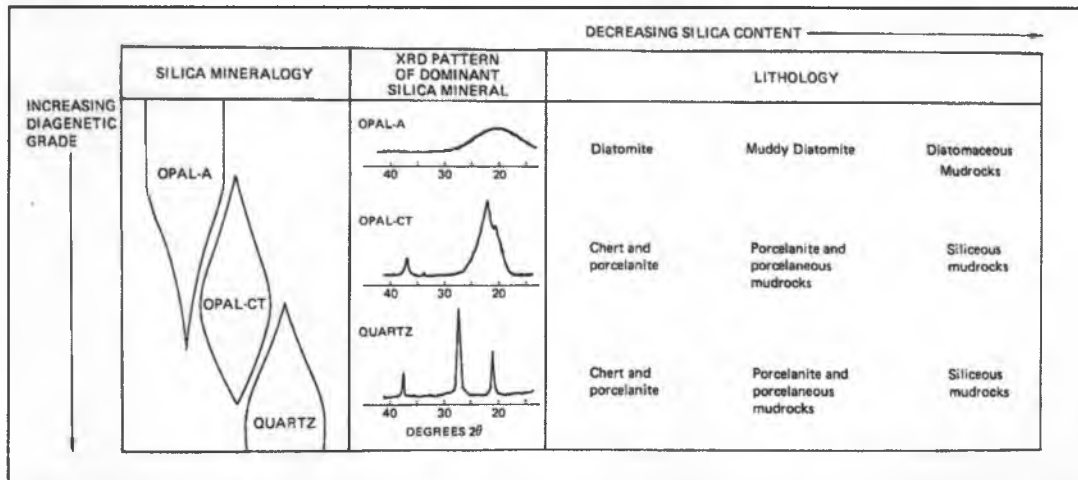


Figure 8. Silica transformation of lithologic units and XRD signals of silica minerals in the Monterey Formation (Pisciotta and Garrison, 1981).

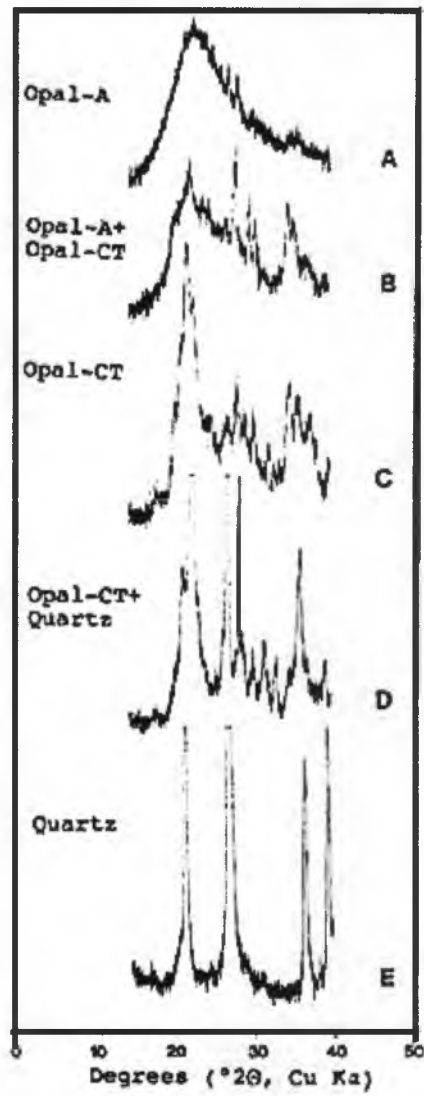


Figure 9. Examples of XRD pattern for silica minerals (from Littke et al., 1991).

4.0. Results

4.1. Stratigraphy of the Point Reyes Structural Block

The following descriptions of stratigraphic units in the Point Reyes area are mostly summarized from previous maps and reports (Galloway, 1977; Clark and Brabb, 1978; and Clark et al., 1984). However, the description of the Monterey Formation is a synthesis of a broader body of information that incorporates my detailed field observations and laboratory data together with information from published reports. The stratigraphic nomenclature of Galloway (1977) for the Point Reyes area was later revised by Clark et al. (1984) and Clark and Brabb (1997) based on their correlations of Tertiary units with sedimentary rocks in the Santa Cruz Mountains and the Monterey area. The nomenclature used herein reflects these later revisions.

Cretaceous Units

In the Point Reyes region, Salinian basement rocks are bound to the northeast by the SAFZ and exposed along Inverness Ridge northward to Tomales Point and comprise Late Cretaceous intrusive rocks and minor host metamorphic rocks of unknown age. As identified by Galloway (1977) and adopted by Clark and Brabb (1978), the Salinian rocks are divided into the tonalite of Tomales Point, granodiorite and granite of Inverness Ridge, and porphyritic granodiorite of Point Reyes. K-Ar (hornblende) ages from rocks near Bodega Head, presumably part of the tonalite indicate an early-Late-Cretaceous age of 94.3 Ma (Evernden and Kistler, 1970). Similar, Late Cretaceous K-Ar ages of 86.8 ± 7.4 and 82.7 ± 6.9 Ma were obtained from biotites in the porphyritic granodiorite (Ross 1978). Enclaves of Paleozoic or Mesozoic metasedimentary rocks are locally mapped in the Salinian intrusive rocks and consist of a variety of rock types including quartzite, mica schist, graphitic marble, quartzofeldspathic gneiss and granofels (Ross,

1977, 1978). The lithologically distinguishable porphyritic granodiorite of Point Reyes is correlated to the porphyritic granodiorite of Monterey exposed at Point Lobos. Averaged initial Sr isotope ratios for the correlative plutonic rocks in these two areas are nearly identical (Clark et al., 1984; Dickinson et al., 2005).

Eocene Units

The Point Reyes conglomerate of Galloway (1977) rests nonconformably upon the porphyritic granodiorite of Point Reyes. The unit is only present in the vicinity of the Point Reyes lighthouse where it is well exposed in seacliffs. The unit consists of thickly interbedded sandy pebble-cobble conglomerate and sandstone. Cobble and pebble lithologies are mostly porphyritic granodiorite (similar to the underlying porphyritic granodiorite of Point Reyes), dark, silicified, well-rounded porphyritic volcanic rocks, and lesser amounts of quartzite, red chert, and light gray and greenish gray volcanic rocks. The conglomerates of Point Reyes are correlated to the conglomerates of Point Lobos (a.k.a., the Carmelo Formation) on the east side of the SGFZ (Clark et al., 1984; Bachman and Abbott, 1988; Burnham, 1999; Figure 3). The conglomerates in both areas have nearly identical relative percentages of clast types; porphyritic rhyolite felsite clasts from both areas have yielded indistinguishable Late Jurassic U-Pb ages of 151.6 ± 2.6 Ma (Burnham, 1999), and both areas contain correlative successions of early Eocene foraminiferal faunas (Kristin McDougall, 1997, personal comm., *in* Dickinson et al., 2005).

Miocene Units

The Laird Sandstone rests nonconformably upon the porphyritic granodiorite of Point Reyes, and on tonalite of Tomales Point. The unit consists of thickly-bedded, medium-to-fine-grained, grayish-tan, generally non-calcareous, arkosic sandstone. The lower part of the unit includes many conspicuous ellipsoidal and irregular-shaped,

calcareous concretions. The nonconformable, basal contact of the unit is well exposed at Kehoe Beach and is marked by a distinct, calcareous, bioclastic pebble and cobble conglomerate resting on an irregular, channelized erosional contact with Salinian granitic rocks. Clast lithologies in the conglomerate include mostly granitic rocks with common quartzite pebbles. Bioclasts in the basal conglomerate consist mainly of mollusks and echinoderms of Luisian (Middle Miocene) age (Clark and Brabb, 1997). The channelized and bioclastic nature of the basal conglomerate resemble tidal channel deposits along an abrasion platform and more clearly represent the initial deposits of a marine transgression marking Laird Sandstone deposition.

The Laird Sandstone is approximately 64m thick where it exposed at Kehoe Beach and it thins east, toward Lairds Landing (Figure 7) and to the south where mapped along the west and south flanks of Inverness Ridge and Tomales Bay (Clark and Brabb, 1997). The thin yet continuous nature of the Laird Sandstone and transitional relation with the clastic-rich strata in the lowermost strata in the overlying Monterey Formation suggest that the Laird Sandstone was deposited on an erosional surface of low relief and that there was little or no opportunity for erosion of the Laird Sandstone prior to deposition of the Monterey Formation.

The Laird Sandstone in the Point Reyes area is correlated to the lithologically similar "Unnamed Sandstone" in the Monterey region (Clark et al., 1984). In both regions the sandstone also shares the same gradational stratigraphic relation with lowermost strata of the overlying Monterey Formation.

Monterey Formation (of Point Reyes)

The lower part of the Monterey Formation is best exposed at Kehoe Beach. It consists of medium-bedded, silty mudstone and thin-bedded siliceous mudstone which are light in color, porous, detrital-rich and locally cherty, and does not express any

biogenic texture (Figures 13 and 14). It is estimated to be 150-m-thick, and rests conformably upon the Laird Sandstone. Approximately 28 m of the total estimated thickness of the lower Monterey was measured in the field at Kehoe Beach. Benthic foraminiferal fauna, including *Florilus costiferus*, *Valvulineria miocenica*, and *Valvulineria californica*, were identified in the section by Clark et al. (1984), and indicate a Luisian (Middle Miocene) age.

According to Clark et al. (1984), the middle section of the Monterey Formation is 450-m-thick, and composed of thin-bedded, pale orange to white porcelanite with laminated shale and biotitic arkosic sandstone interbeds. They are typically very light-gray or light-brownish-gray, and laminated. Most lithologies in this area can be scratched with a knife, but harder undeformed chert nodules and chert interbeds are also present locally. Monterey Formation mapped southeast of Kehoe Beach and north of Sculptured Beach is lithologically undefined in previous reports. The Monterey member deposited between Laird and Santa Margarita sandstone formations is the thinnest north of Drakes Bay. Based on the benthic foraminiferal fauna dating result of Galloway (1977) and Clark et al. (1984), this thin Monterey section is mostly Mohnian stage, and may be in part equivalent to the section measured at Sculptured Beach.

Clark et al. (1984) determined the thickness of the upper section as 450 to 900-m-thick. The section consists of interbedded light-colored porcelanite with dark, brittle chert, and dark brown mudstone interbeds. Approximately over 40 m of the upper section of the Monterey Formation that strikes averagely N60W and no specific dip direction or attitude due to highly contorted strata. The top of the section is composed mainly of highly contorted cherts, approximately 100 m-thick (White, 1989); they are brown to black in color, vitreous, cannot be scratched with a knife, and express rarely chert nodules (Figures 16 and 17). There are distinctive chert spheroids well exposed

Sculptured Beach. Also, an angular unconformity between the top of the upper section and Santa Margarita Sandstone is visible at this area.

White (1989) indicates that the chert facies are not time equivalent between Point Reyes in the Bodega Basin, northern central California coast, and the Santa Maria Basin on the southern California coast, having younger chert facies. This nonconcurrent chert distribution along the California coast gives us a good constraint about variation in temperature and onset of upwelling from north to south. The Monterey Formation within the area is predicted to be as much as 1500 m thick, and the presence of the benthic foraminifers are interpreted as indicators of bathyal or greater depths, and Middle and Late Miocene (Luisian and Mohnian) age by Clark et al., (1984).

The Santa Margarita Sandstone rests nonconformably on the Monterey Formation in the study area. The angular unconformity between the Santa Margarita Sandstone and the Monterey Formation is clearly exposed at Sculptured Beach at Point Reyes. Middle to fine grained arkosic sandstone is bituminous and bioturbated near Sculptured Beach and Double Point. The thickness of the sandstone unit varies from 8 to 60 m (Clark et al., 1984). Megafossils collected from the bottom of the section suggest a Late Miocene age for the formation (Bowen, 1965).

Santa Cruz Mudstone conformably overlies the Santa Margarita Sandstone. The formation consists of light-gray to light-yellowish-gray, thin-to thick-bedded and laminated, siliceous mudstone. It locally includes calcareous concretions (Clark et al., 1984). Southeast of Double Point, bituminous sand inclusions are exposed at the base of the mudstone. The thickness of the Santa Cruz Mudstone in the Point Reyes area varies from 1040 to 2000 m in the offshore areas between the Duxbury Point and Bolinas. The maximum exposed thickness of the formation is clearly in the southernmost part of the Point Reyes block in the area just north of Bolinas but the exact thickness is difficult to determine due to poor exposures and extensive landslides in this area. The Santa Cruz

Mudstone in the Point Reyes area earned its name from its correlation to strata in the type area of the formation, the Santa Cruz Mountains where the formation is reported to be up to 2300 m thick (Clark and Brabb, 1978). Diatom flora and calcareous benthic foraminifers from the formation are indicative of a Late Miocene age for the Santa Cruz Mudstone (Clark et al., 1984).

Miocene to Pliocene Units

The Purisima Formation resting conformably upon the Santa Cruz Mudstone, consists of thick-bedded, yellowish gray, and diatomaceous siltstone. The commonly bioturbated Purisima Formation includes spheroidal carbonate concretions. It has at least nearly 490 m in thickness where the broad Point Reyes synclinal is present at Drakes Bay (Clark et al., 1984). A diatom flora and the pinniped fauna are indicative of the latest Miocene to Pliocene age for the Purisima Formation. Repenning and Tedford (1997) suggests that it deposited between 6 and 4 Ma. According to Clark et al. (1984), lower part of the formation, first 40 m, is Late Miocene age; whereas, upper part of the unit is Pliocene age even though it was not dated well. It is correlative with Purisima section exposed on the Santa Cruz Mountains (Clark, 1981).

Quaternary Deposits, undifferentiated

They consist of terrace deposits, older dune sands, landslide deposits, alluvium, dune sands, and beach sands in the area. Deposits range in age from early Pleistocene to Holocene (Clark et al., 1984).

4.1.1. Cross Sections and Stratigraphic Column Constructed

I built four cross sections in the Point Reyes area. The location map and cross-sections are shown in Figures 11, 12, 15, 18 and 19. My field observations and cross-

sections helped me estimate the minimum thicknesses of the lithologic units in the area (Table 4). I then established a stratigraphic column of the units in my sampling locations extending from Sculptured Beach to the north of Drakes Bay and up to Kehoe Beach (Figure 22). I compared my stratigraphic column with the generalized stratigraphy of Clark et al. (1984) for the region (Figure 10).

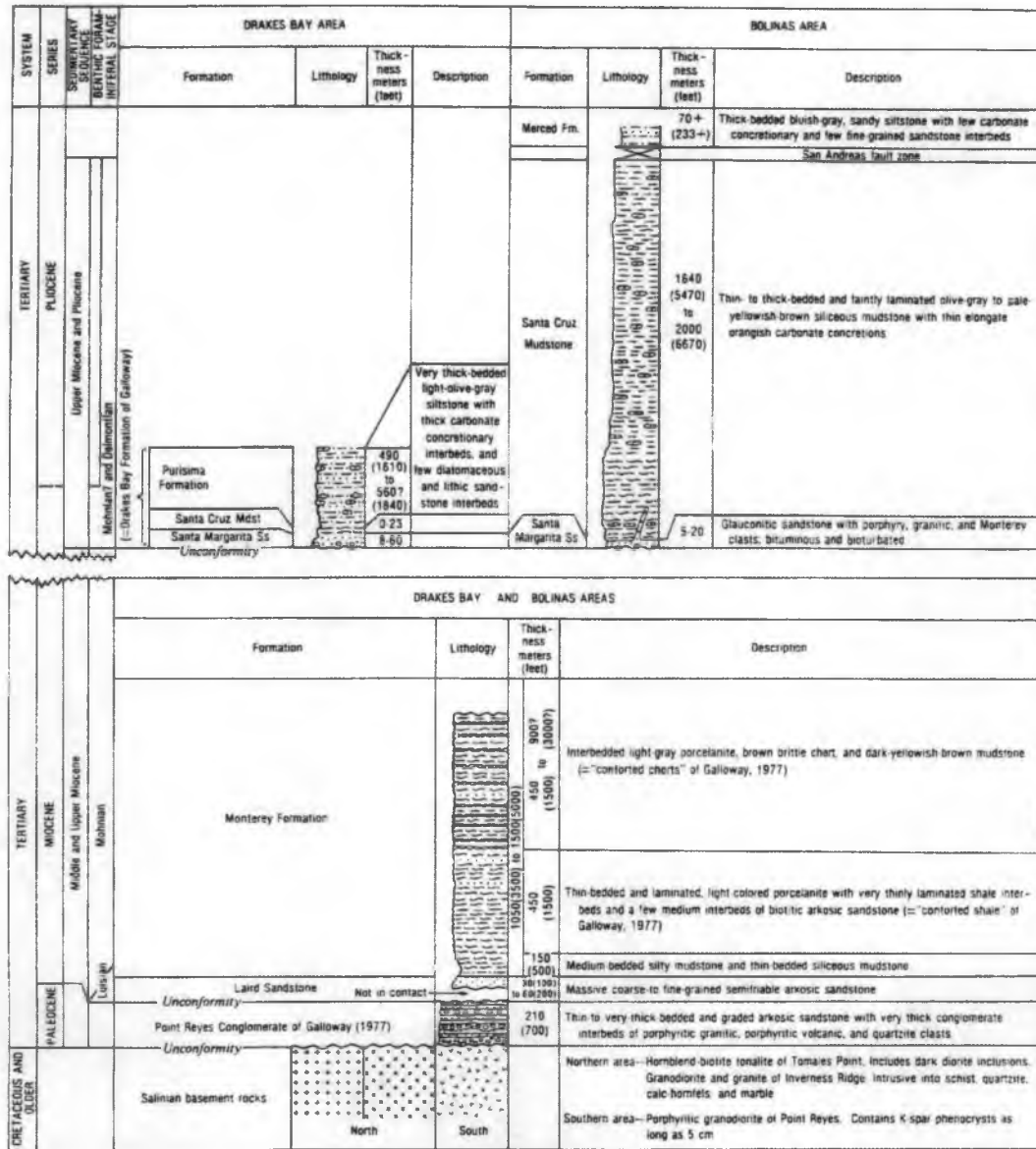


Figure 10. Generalized stratigraphy of the Point Reyes area (from Clark et al., 1984).

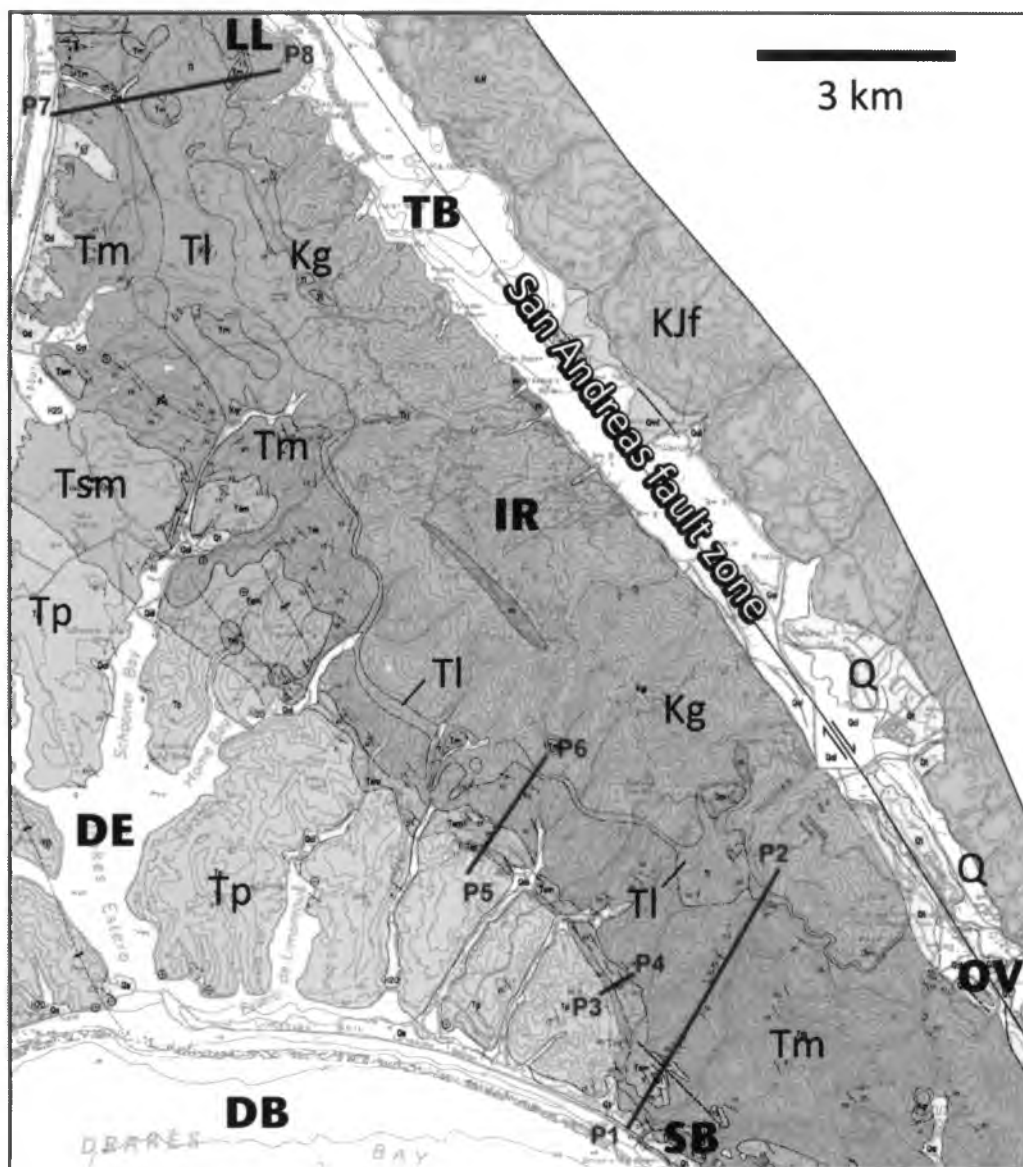


Figure 11. Geologic map of the central part of the Point Reyes structural block (from Clark and Brabb, 1997) showing the locations of the four cross sections (bold red lines) that were constructed for the Point Reyes study area. Geologic units: Jurassic-Cretaceous: KJf— Franciscan Complex; Kg—Cretaceous granitic rocks; Miocene rocks: Tl—Laird Sandstone; Tm— Monterey Formation; Tsm— Santa Margarita Sandstone; Pliocene: Tp— Pliocene Purisima Formation; Quaternary: Q—undifferentiated Quaternary.

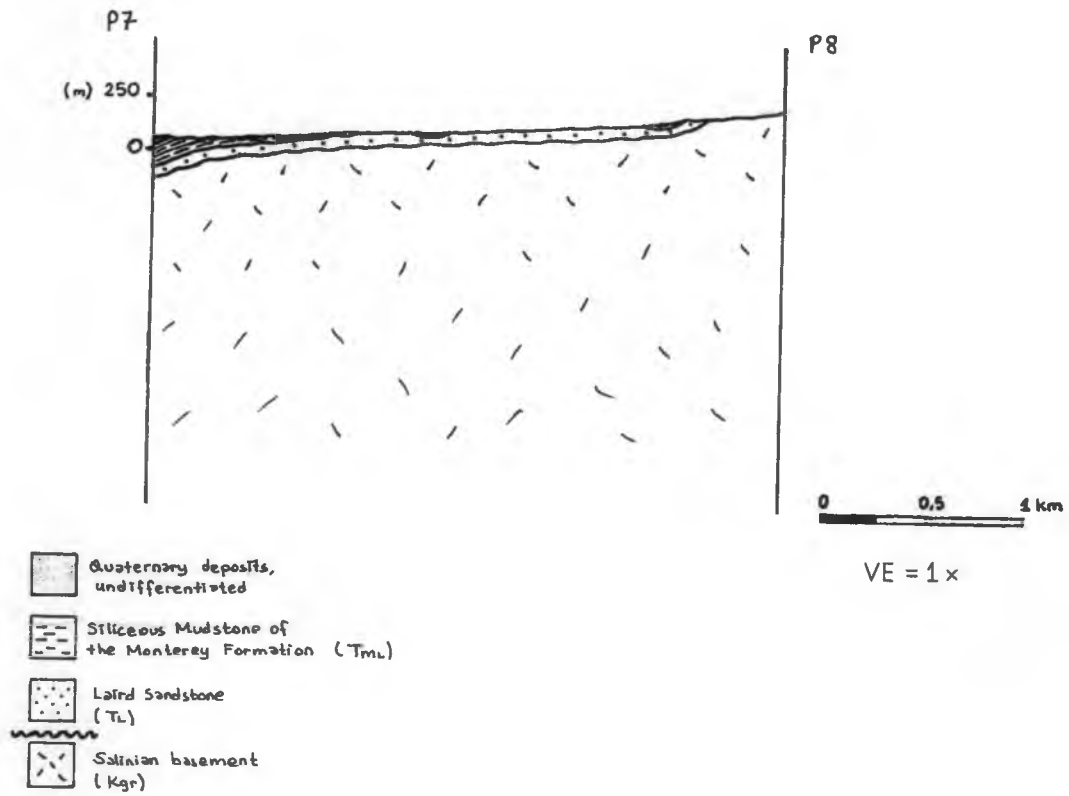


Figure 12. Southwest-northeast cross section P7—P8, Kehoe Beach to Tomales Bay, Point Reyes area (see Figure 11 for location).



Figure 13. Siliceous mudstone exposure of the Monterey Formation at Kehoe Beach, Point Reyes.



Figure 14. Siliceous mudstone samples, 8.1.T and 8.6, collected from the Kehoe Beach, Point Reyes (Table 2).

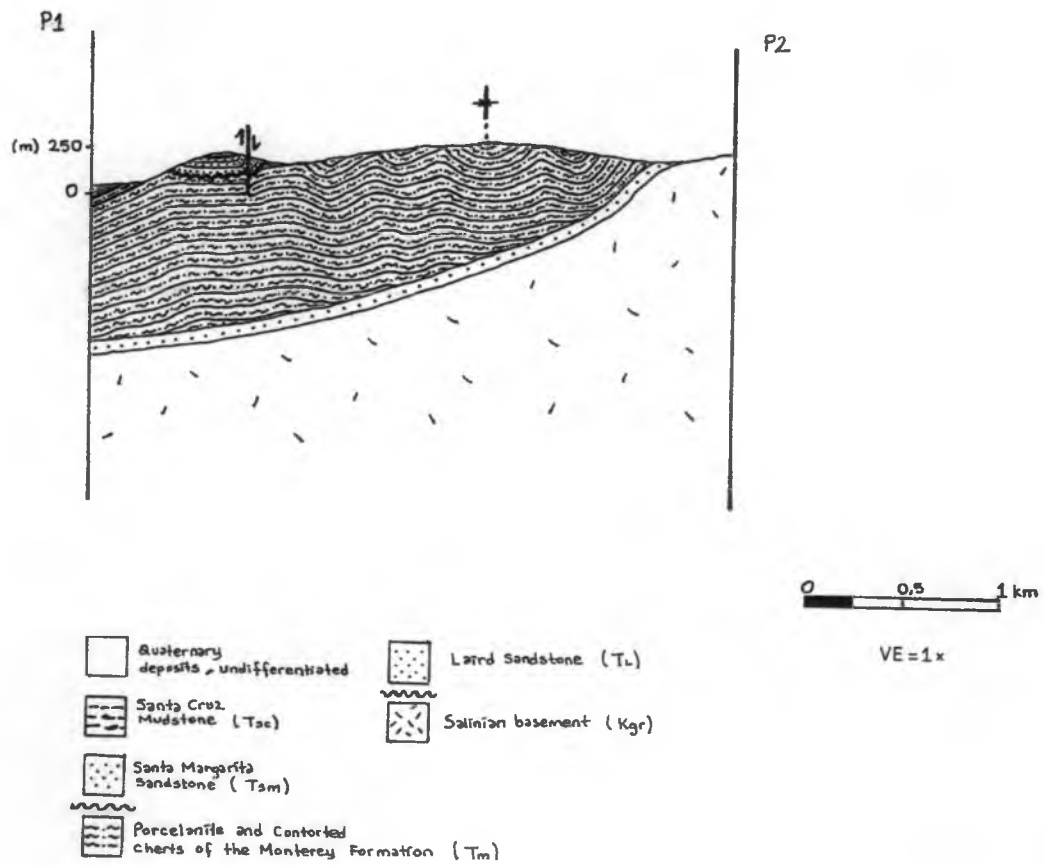


Figure 15. Southwest-northeast cross section P1—P2, Sculptured Beach area (see Figure 11 for location).

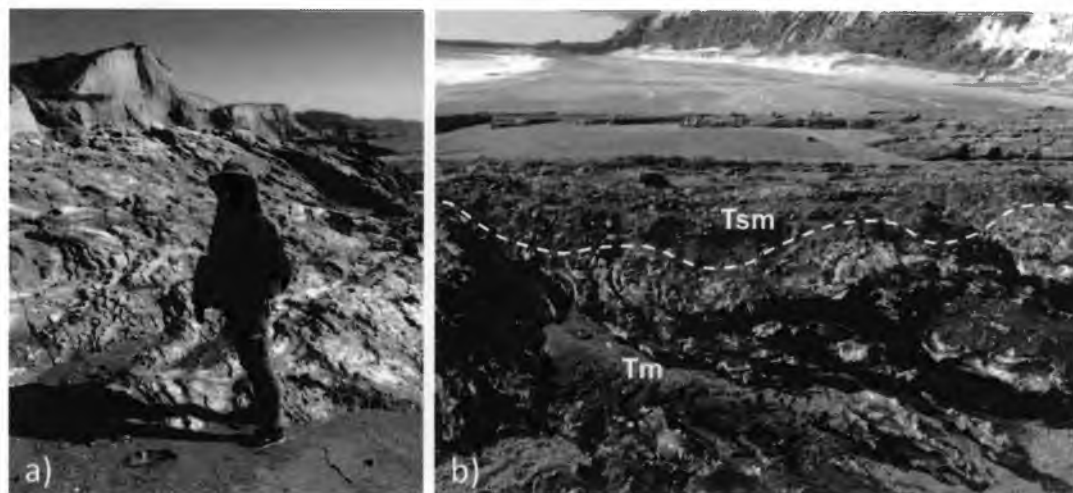


Figure 16. Exposures at Sculptured Beach, Point Reyes area (Figure 11) showing: a) view to south of highly-contorted chert , cherty-porcelanite, and dolomite of the Monterey Formation, and b) view north of the well-exposed angular unconformity (white dashed line) between the basal conglomerate of the Santa Margarita Sandstone (Tsm) and contorted layering of the Monterey Formation (Tm).



Figure 17. Black chert sample on the left, 9.3, collected from Sculptured Beach, light gray chert sample in the middle, 9.4, collected north of Sculptured Beach, and gray porcelanite sample on the right, 9.1, collected from Sculptured Beach, Point Reyes (Table 2).

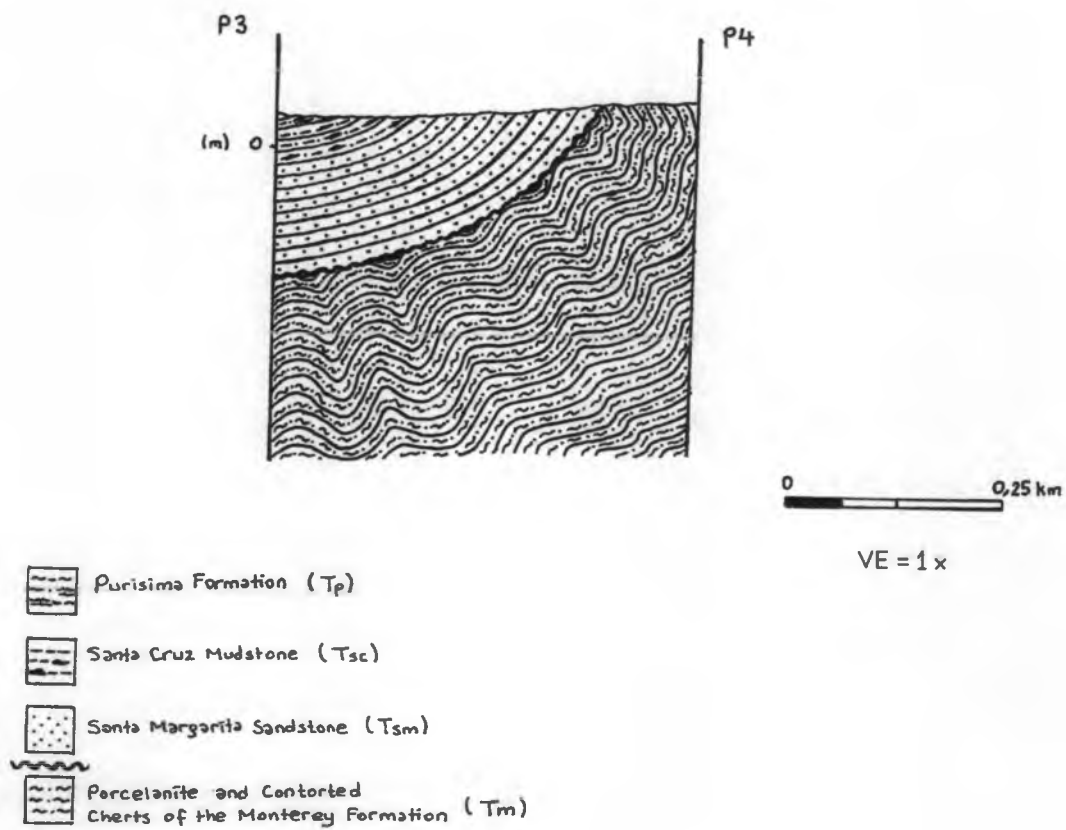


Figure 18. Southwest-northeast cross section P3—P4, north of Sculptured Beach area (see Figure 11 for location).

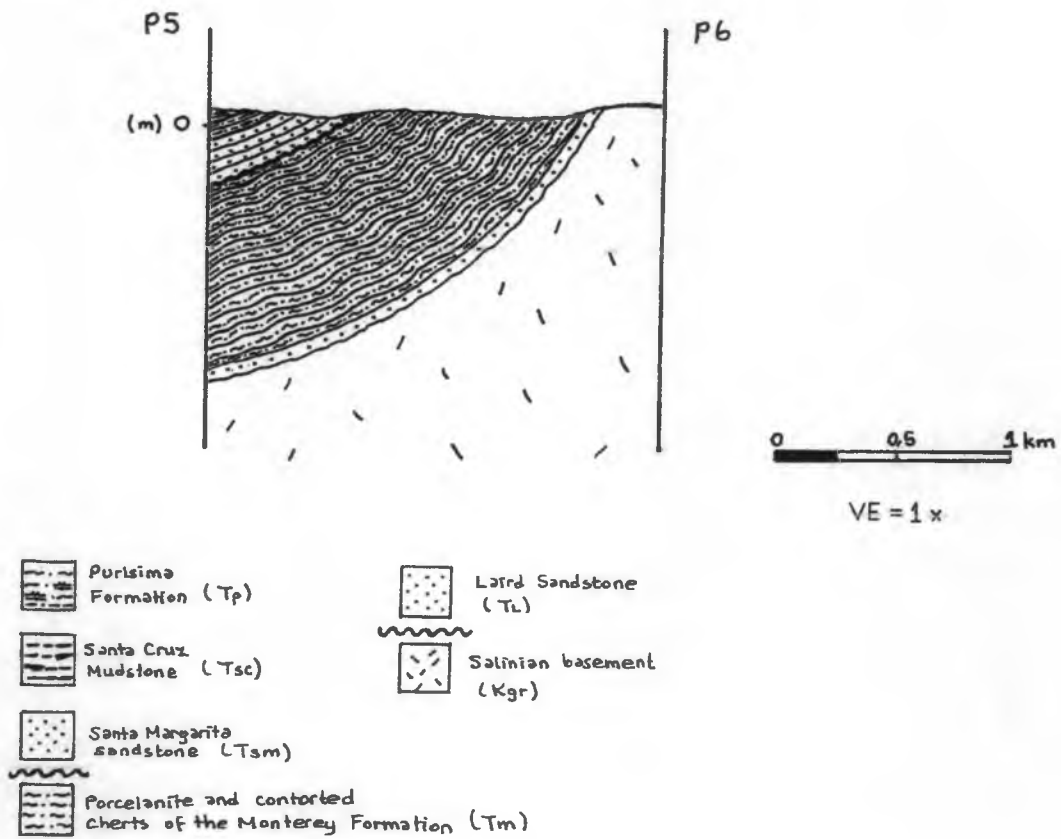


Figure 19. Southwest-northeast cross section P5—P6, north of Drakes Bay area (see Figure 11 for location).



Figure 20. Porcelanite exposure of the Monterey Formation north of Drakes Bay, Point Reyes.



Figure 21. Porcelanite sample, 3.1, collected north of Drakes Bay area, Point Reyes (Table 2).

Table 4. Estimated minimum thicknesses of the lithologic units in my cross sections in the Point Reyes Area

Lithologic unit	Estimated thickness (m)	Clark's estimations (1984) (m)
Purisima Fm. (Tp)	17 to 45	490 to 560
Santa Cruz mudstone (Tsc)	19 to 45	0 to 23
Santa Margarita sandstone (Tsm)	78 to 130	8 to 60
Cherty porcelanite of Monterey (Tm)	667 to 773	900 to 1350
Siliceous mudstone of Monterey (Tml)	80	150
Laird sandstone (Tl)	45 to 56	30 to 60

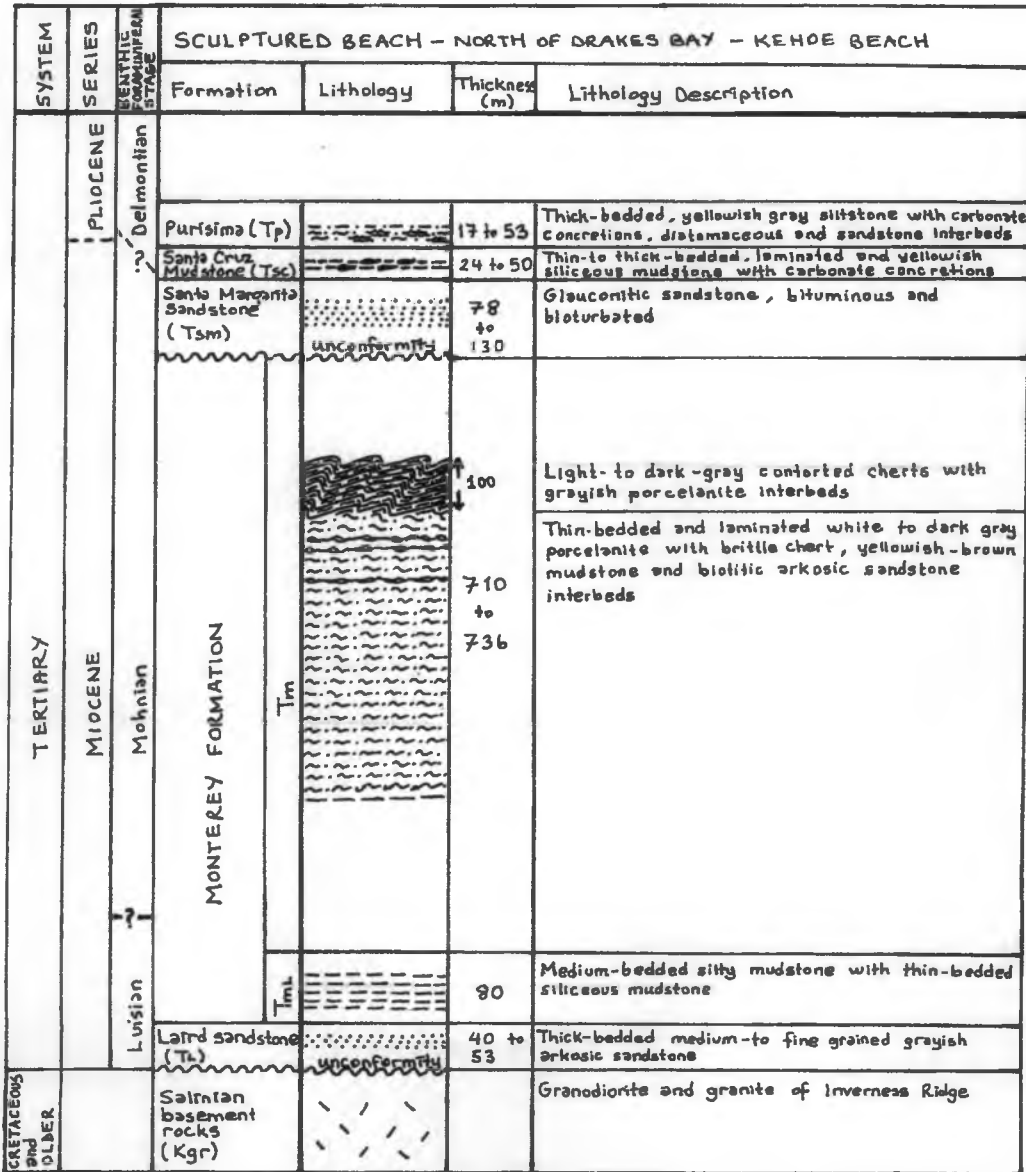


Figure 22. Stratigraphic column of the Sculptured Beach, north of Drakes Bay and Kehoe Beach, Point Reyes.

4.1.2. Petrographic Analysis of Silica on Monterey Formation

I did petrographic analyses of six thin sections from the sampling locations at Point Reyes; I made thin sections of samples 8.1.T, 8.6, 9.5, 9.4, 9.3, and 9.2 (Table 2). I estimated the amount of detrital quartz by comparing this with the quartz peaks in XRD patterns. In addition I estimated the amount of biogenic silica; opal-A, opal-CT and quartz, which all look dark under polarizing light microscope as compared to a whitish birefringence for detrital quartz grains.

8.1.T has a high amount of detrital quartz and feldspar grains, and there is no carbonate is present. Likewise, 8.6 is rich in detrital quartz and feldspar grains, but carbonate is present. Both samples have nearly %25-35 biogenic silica; however, there are no diatoms or benthic foraminifer visible. 9.5 has approximately %50 biogenic silica and detrital quartz. 9.4 and 9.3 have approximately %80-90 biogenic silica, feldspar and a small amount dolomite. 9.2 has about %60-70 biogenic silica, and the remainder is mainly dolomite.

4.1.3. X-Ray Mineralogy of Silica on Monterey Formation

I ran twelve samples from the Monterey Formation that I collected from different locations at Point Reyes (Table 2). I compared the XRD patterns of samples having opal-A, opal-CT, or microcrystalline quartz as the major silica phases, in previous studies, shown in Figures 8 and 9, with diffraction patterns of my samples. This qualitative comparison is mainly based on the values of intensity, scattering angle (2θ), and size and shape of each peak in XRD signals of my samples and the values of the peaks in the samples of previous studies mentioned above.

The XRD pattern of 8.1.T reveals a distinctive quartz signal. However, the quartz signal cannot differentiate between detrital and biogenic quartz of the sample. Based on my hand specimens, field observations, petrographic analysis, and Isaacs and Kelham (1985) diagram (Figure 6), I can say that the sample of the siliceous mudstone member has approximately %30 biogenic silica, and approximately %70 detrital constituents, largely clay minerals, and small amount of Tridymite. I can suggest that the most of quartz in the sample are detrital quartz. While thin section analysis of the same sample, 8.1.T, supports nearly %30 biogenic silica presence, its XRD pattern suggests that the all biogenic silica should be quartz since there is neither opal-A nor opal-CT signal in the pattern (Appendix A.1). Likewise, sample 8.6 has a similar quartz signal with considerable amount of calcite, and most of the quartz appears to be detrital. (Appendix A.2).

8.1.T.1, and 8.1.T.2 have opal-CT as a major phase. I estimate nearly %30 biogenic silica, along with additional detrital quartz and clay minerals (Appendices B.1 and B.2). Samples 9.5, 7.1, 6.1, and 3.1 have opal-CT as the most dominant phase comprising nearly %50 of the rock. Additionally, the XRD shows detrital quartz and clay minerals are also present. (Appendices C.1, C.2, C.3 and C4). Samples 9.4, and 9.3 have opal-CT as the major phase with nearly %80-90 biogenic silica along with a minor amount of detrital quartz indicated by sharp quartz peaks (Appendices D.1 and D.2). Sample 9.2 has distinctive dolomite peaks, but opal-CT is the major phase with nearly %60-70 biogenic silica along with a few sharp peaks indicating a minor amount of detrital quartz (Appendix C.5).

Most of the samples collected contain opal-CT as the major biogenic silica phase. The final sample, 9.1, has a quite different pattern from other samples. Even though the pattern looks very similar to the quartz pattern, all of sharp peaks are dolomite, and it has negligible amount of quartz, and opal-CT. I collected this sample from the area having

cherty porcelanites, and I believe that this sample is most likely coming from the dolomite beds in the section (Appendix E.1). Overall the major silica phases present in the samples analyzed are shown in Table 5 and Figure 38.

Table 5. XRD results of the Monterey Formation samples in the Point Reyes area

Sample ID	Lithology	Major silica phase
8.1.T	siliceous mudstone	quartz
8.6	siliceous mudstone	quartz
8.1.T.1	siliceous mudstone	opal-CT
8.1.T.2	siliceous mudstone	opal-CT
9.5	porcelanite	opal-CT
7.1	porcelanite	opal-CT
6.1	porcelanite	opal-CT
3.1	porcelanite	opal-CT
9.4	gray chert	opal-CT
9.3	black chert	opal-CT
9.2	porcelanite-bituminous sand contact	opal-CT
9.1	cherty porcelanite	dolomitic

4.2. Diagenetic History of the Monterey Formation at Point Reyes

The lower part of the Monterey section at Kehoe Beach at Point Reyes include both opal-CT and quartz phase biogenic silica. Two samples, 8.1.T and 8.6, have been buried deeper than the other two samples, 8.1.T.1 and 8.1.T.2, based on superposition. These two more deeply buried samples contain approximately %30 biogenic quartz since there is no opal-A or opal-CT signal in the XRD pattern. This supports my contention that the siliceous mudstone section at Kehoe Beach has been buried deeper, reaching the depths required to transform opal-CT to biogenic quartz (Table 5).

When we look at the diffraction patterns of the other two samples, 8.1.T.1 and 8.1.T.2, opal-CT appears to be the major silica phase. This suggests that they have not been buried deep enough to convert opal-CT to quartz. However, they must have almost reached the burial depth required for opal-CT to quartz transformation since they are in the upper part of the nearly 80-m-thick siliceous mudstone section.

The upper member of the Monterey Formation exposed at Sculptured Beach is relatively low in detritus and high in biogenic silica compared to the lower member. The member is in the opal-CT zone, and has not been buried deep enough to convert opal CT to quartz. Opal-CT porcelanite was formed as the result of diagenesis of the primary muddy diatomite, and contorted opal-CT cherts on top of the porcelanite were directly transformed from pure diatomites. The approximately 100 m-thick contorted chert section in the region must have undergone temperatures of nearly at least $\sim 42^{\circ}\text{C}$ (Figure 6) to form the distinctive chert structures, dikes and brecciations that we see today at and east of Sculptured Beach (Figure 16). As a special case, rare opal-CT chert nodules exposed at Sculptured Beach may have originally formed at lower temperatures within diatomite by silica addition.

4.2.1. Estimated Burial Depths of the Monterey Formation

The estimated burial depth gives us a good idea of the temperature required to convert the section to quartz phase, and can be estimated by dividing the burial temperature by the approximate geothermal gradient during the timing of diagenesis. Past-geothermal gradients control the burial depth of silica transformations. For these calculations, I used the present-day geothermal gradient values for California basins. Two scenarios were considered during these calculations. The first case is that the Monterey Formation today exposed in the Point Reyes and Monterey areas underwent diagenesis

under the range of typical geothermal gradients of coastal California which is between 25°C and 50°C (MacKinnon, 1989; Brink et al., 2000). The second case is that the Monterey Formation in these locations underwent diagenesis under higher geothermal gradient, 55°C, than the range given above because the plate motions and migrating Mendocino Triple Junction (MTJ) apparently formed a slab window resulting in high heat flow during the time of diagenesis around the Santa Cruz area; this would facilitate silica transformation at relatively shallower depths (Crouch and Suppe, 1993; Nicholson et al., 1994). I also assumed that the surface temperature is 15°C, and entire section is diatomaceous.

There is an angular unconformity (erosional surface) between the contorted chert and the overlying unfolded Santa Margarita Sandstone. It appears that the overlying rock thickness was insufficient to result in opal A to opal CT conversion. Therefore silica transformation must have occurred before Santa Margarita deposition, and the overburden pressure must come from the Monterey Formation, much of which has been eroded away. This is clearly shown in the nearby seismic section shown in Figure 24.

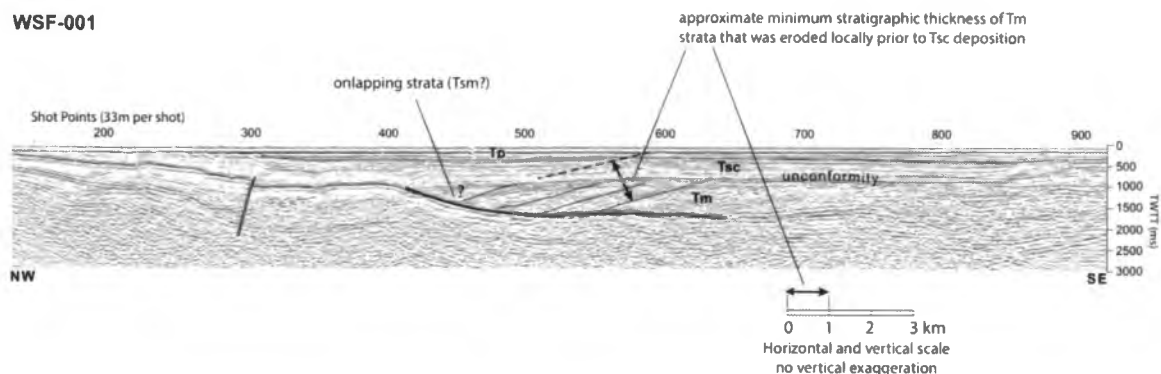


Figure 24. Profile image of WSF-001 seismic line, which is oriented parallel to the Point Reyes coastline from Bolinas to Drakes Bay (see Figure 23 for location). Colored lines are from Stozek (2012); red and yellow—faults east of Point Reyes, green—unconformity at base of the Santa Cruz Mudstone (Tsc), blue—unconformity at base of the Purisima Formation (Tp). Other abbreviations: Tm—Monterey Formation; Tsm—Santa Margarita; TWT—two-way travel time. The image is annotated to show stratigraphic layering in Tm where truncated below an angular unconformity beneath Tsc and Tsm (?). An estimate of ~1000 m of Tm strata appear to be eroded at the unconformity (image modified after Stozek, 2012).

My calculations suggest that the range of the minimum burial depth for the entire Monterey section in the Point Reyes area is approximately between 1138 and 2000 m., and the range of erosion was nearly 391 to 283 m (1138 m – (747 to 853)).

Table 6. The Ranges of minimum burial depths of the Monterey Formation members, Point Reyes. The thickness of chert was provided from White (1989), and the minimum burial temperatures from Figure 6.

Surface temp. (°C)	Thermal gradient (°C/km)	Monterey members	Min. estimated thicknesses (m)	Min. burial temp. (°C)	Estimated burial depths (m)	Min. burial depths (m)
15	25	Chert	100	42	1080	2000
		Porcelanite + Siliceous mudstone	647 to 753	65	2000	
	50	Chert	100	42	540	1187 to 1293
		Porcelanite + Siliceous mudstone	647 to 753	65	1000	
	55	Chert	100	42	491	1138 to 1244
		Porcelanite + Siliceous mudstone	647 to 753	65	909	

4.3. Stratigraphy of the Monterey Area

Like the stratigraphy section of the Point Reyes area, only the stratigraphy of the Monterey Formation is incorporated with my detailed field observations and field and laboratory data; the stratigraphic features of the other units were summarized using previous studies for the Monterey area (Figure 25).

Cretaceous Units

Salinian Basement rocks are exposed as two types of granitic rocks in the Monterey area, Granodiorite of Cachagua and Porphyritic Granodiorite of Monterey. Granodiorite of Cachagua is well exposed near Laureles Grade, and Late Cretaceous Porphyritic Granodiorite of Monterey exposed on the Monterey Peninsula and the south of Carmel Valley.

Eocene Units

The Carmelo Formation of Bowen (1965) nonconformably overlies the granodiorite or is faulted against the granitic basement in many places. According to Clark et al. (1984), the 220-m-thick Carmelo Formation consists of thick bedded, graded arkosic sandstone with interbedded siltstone and cobble and pebble conglomerate. The presence of mollusks and foraminifers are diagnostic of the age of Paleocene for the formation (Bowen, 1965).

Oligocene Units

The Carmeloite of Lawson (1893) crops out near Carmel Bay and east of Carmel Valley, and unconformably rests upon the granodiorite or locally faulted against it. The 20-m-thick unit is mainly composed of basalt. The result of the K-Ar dating suggests the age of 27 ± 0.8 Ma, Oligocene time, for the Carmeloite Formation (Clark et al., 1984).

Miocene Units

The Red Beds of Robinson Canyon rest nonconformably above the Salinian granite and below the Monterey Formation in Robinson Canyon. The rocks consist of red, non-marine, coarse grained arkosic sandstone with red, thin siltstone and conglomerate beds with thick beds of well-rounded cobbles (Bowen, 1965). Middle

Miocene age Red Beds is approximately 140 m thick in Robinson Canyon (Younse, 1980).

The Los Laureles Sandstone Member of Bowen (1965) rests conformably upon the Red Beds in Robinson Canyon. It was named as "Unnamed Sandstone" by Clark et al., (1974). This marine sandstone unit consists of light orange, thick bedded, coarse to fine grained arkosic sandstone, and siltstone beds in the upper part, and thick conglomerate beds at the base. Sandstone beds exposed along the Potrero Canyon are approximately 175 m thick, and includes foraminifers at top which are diagnostic of late Luisian (Middle Miocene) age (Clark et al., 1997).

Monterey Formation (of Monterey Area)

The total thickness of the Monterey Formation in the Monterey area is approximately 880 m. Three members are present, designated lower, middle and upper.

The sites that have older siliceous mudstone exposures are limited in the region. The best locations having exposures of the older section extend from Whispering Pines Park to the Carmel Woods area. The 30-m-thick lower member consists of thin, yellowish, semi-siliceous mudstone beds with thin siltstone interbed; the rocks are light in color, porous, detrital-rich, locally porcelaneous; they do not express any biogenic textures, and the section looks quite similar to the lower siliceous mudstone exposed at Kehoe Beach at Point Reyes. It conformably rests upon the Unnamed Sandstone. McDougall (1987) suggested that benthic foraminifers in this unit are indicative of 150 to 350 m water depths, upper bathyal, and of Luisian (Middle Miocene) (Figures 28 and 29).

The middle member is mainly thin bedded, whitish to grayish, laminated porcelanite. The rocks are fine grained, can be scratched with a knife, and has harder, vitreous chert interbeds (Figures 31 and 32). The member is well exposed at Pacific

Meadows Park on the Carmel Valley Road and along Saddle Road. The 600-m-thick section includes benthic foraminiferal faunas, and Younse (1980) interpreted them as being deposited in upper bathyal depths during Luisian (Middle Miocene) time to lower middle bathyal depths during Mohnian (Middle to Late Miocene) time. Unlike the contorted chert in the upper part of the correlative section at Point Reyes, there is no distinctive chertification within the section in the Monterey area.

The upper diatomaceous section, is approximately 250-m-thick, and consists of laminated, yellow to white diatomite with thin, brownish chert and gray vitric tuff interbeds. The diatomite is soft, white in color, porous, chalky, lightweight, and rich in detritus. It is well exposed along Toro Road and Laureles Grade. Radiometric age dating of vitric tuff (McDougall, 1994; Sarna-Wojcicki, 1996) in this upper unit gives 10.83 ± 0.03 million-year old. This is younger than the age of the base of middle porcelanite member, and they should be considered as different members. It also suggests that the diatomites were deposited in a shallowing environment, as there is no unconformity between overlying shallow marine Santa Margarita Sandstone (Figures 34 and 35).

The Santa Margarita Sandstone rest conformably upon the diatomite of the Monterey Formation, is exposed along the Chupines fault zone, north and south of Canyon Del Rey in the study area, where it is 150-m-thick (Clark et al., 1984). It is a marine, light colored, fine to coarse grained arkosic sandstone. According to Herold (1934) and Bowen (1965), megafossil presence in the formation indicates the age of Late Miocene for the Santa Margarita Sandstone.

Pleistocene Units

The Paso Robles Formation rests unconformably upon the Santa Margarita Sandstone, and consists of non-marine, sand and silt beds with light gray gravel beds.

This Pleistocene age formation is about 150 m-thick (Clark et al., 1984), and is mainly exposed at Pacific Meadows Park on the Carmel Valley Road.

Quaternary Deposits, undifferentiated

Quaternary deposits consist of a variety shallow marine and non-marine deposits ranging in age from Pleistocene to Holocene (Clark et al., 1997).

QUA- TERNARY	SYSTEM	SERIES	STAGE	Rock unit	Lithology	Thickness meters (feet)	Description				
								PLEIST.	PLEIST.		
TERTIARY				Aromas Sand		80 (200)	Yellowish-brown to grayish-orange fine sand; nonmarine				
				Paso Robles Formation		150 (500)	Light gray gravel, sand, and clay; nonmarine				
				Santa Margarita (?) Formation		150 (500)	Very thick bedded white coarse- to fine-grained friable arkosic sandstone				
				Canyon del Rey Diatomite Member of Bowen (1965)		250 (830)	Very thick bedded and faintly laminated whitish diatomite with thin interbeds and lenses of waxy-brown opaline chert and with few thick interbeds of gray pumicite (=Tm of Clark and others, 1974)				
				Agujate Shale Member of Bowen (1965)		600 (2000)	Thin-bedded, light brown to white porcelanite with very thin clay shale partings between porcelanite beds and with thin interbeds of waxy-yellow to brown opaline chert. Contains few thin, dark-brown bentonite interbeds and rare thin phosphatic oolite interbeds in lower part (=Tm of Clark and others, 1974)				
				Los Laureles Sh. Mbr. of Bowen (1965)		30 (100)	Thin-bedded yellowish-brown semisiliceous mudstone with interbedded siltstone (=Tm of Clark and others, 1974)				
				Carmelito de Lawson (1893)		80 (200)	Thick-bedded medium- to fine-grained buff-weathering arkosic sandstone (=Tus of Clark and others, 1974)				
				Carmelo Formation of Bowen (1965)		20 (65)	Flows and flow-breccias of basalt. Age 27m.y.				
				<i>Unconformity</i>							
				CRETACEOUS AND OLDER				Salinian basement			Porphyritic granodiorite of Monterey with K-feldspar phenocrysts 3 to 10 cm long to south and east, grades through granodiorite (Cachagua mass of Ross, 1976) into hornblende-biotite quartz diorite (Soberanes Point mass of Ross, 1976)

Figure 25. Generalized stratigraphy of the Monterey area (from Clark et al., 1984).

4.3.1 Cross sections and Stratigraphic Column Constructed

Like the method I followed for the Point Reyes calculations, I constructed four cross sections in the Monterey area. Location map and cross-sections constructed are shown in Figures 26, 27, 30, 33 and 36. I then used them to estimate the minimum thicknesses of the lithologic units in the area (Table 7), and to establish a stratigraphic column of the units in my sampling locations (Figure 37). I compared my stratigraphic column with the generalized stratigraphy of Clark et al. (1984) for the region (Figure 25).

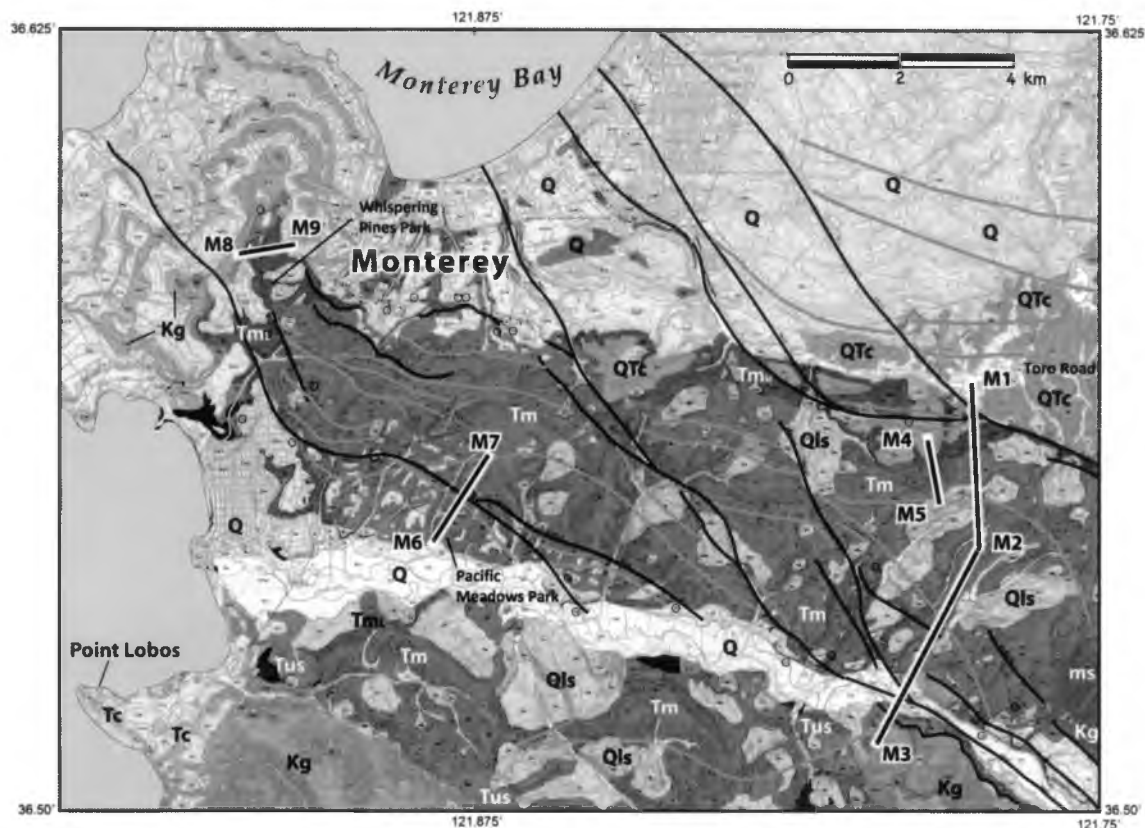


Figure 26. Geologic map of the part of the Monterey area (from Clark et al., 1997: U.S.G.S. Digital Database) showing the locations of four cross sections (red lines) that were constructed for the Monterey study area. Geologic units: Pre-Cretaceous and Cretaceous: ms—Schist of Sierra; Kg—granitic rocks: Eocene rocks: Tc—Carmelo Formation: Miocene rocks: Tus—Unnamed Sandstone; Tml—lower siliceous mudstone of the Monterey Formation; Tm—middle porcelanite of the Monterey Formation; Tmu—upper diatomite of the Monterey Formation; Tsm— Santa Margarita Sandstone: Quaternary: Q—undifferentiated Quaternary. Green lines represent fold hinge lines, and black lines are fault.

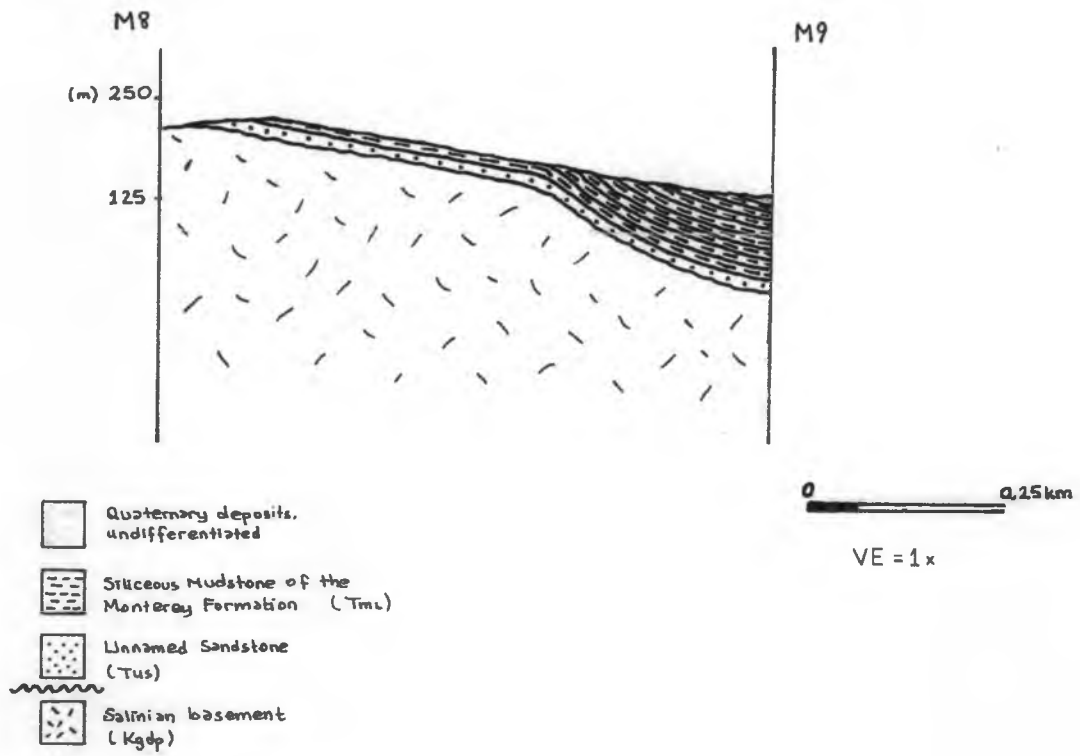


Figure 27. Southwest-northeast cross section M8—M9, northwest of Whispering Pines Park area (see Figure 26 for location).



Figure 28. Siliceous mudstone exposure of the Monterey Formation at Whispering Pines Park, Monterey area.

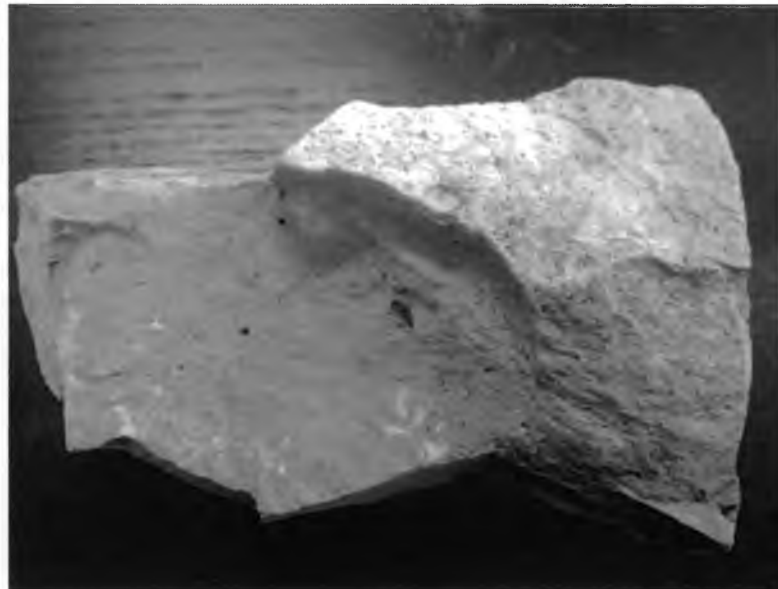


Figure 29. Siliceous mudstone sample, 11.1, collected from the Whispering Pines Park, Monterey area (Table 3).

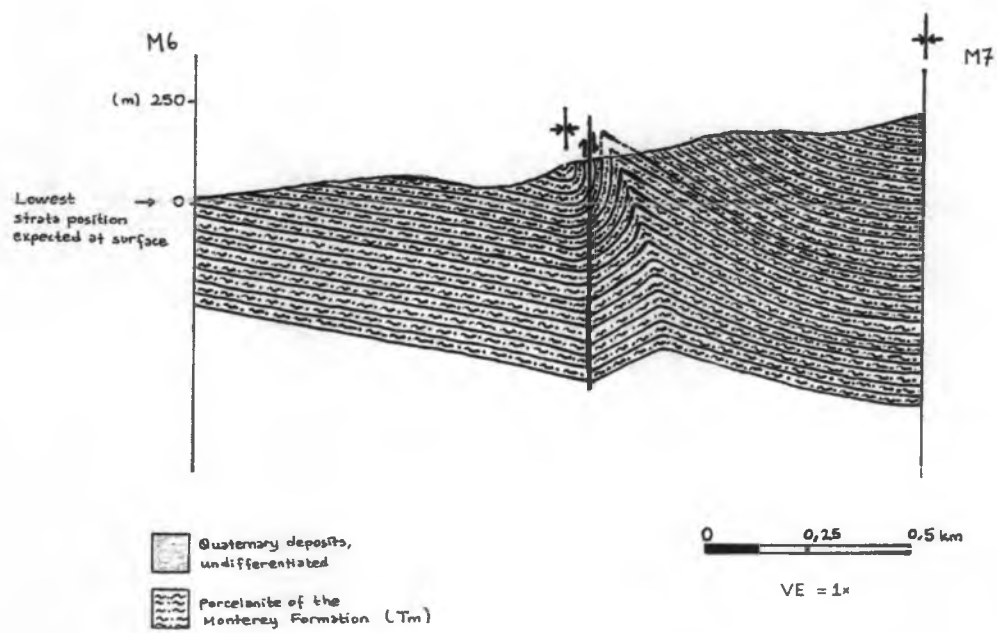


Figure 30. Southwest-northeast cross section M6—M7, Pacific Meadows Park area (see Figure 26 for location).



Figure 31. Porcelanite exposure of the Monterey Formation at Pacific Meadows Park, Monterey area..



Figure 32. Porcelanite sample, 6.1, collected from the Pacific Meadows Park, Monterey area (Table 3).

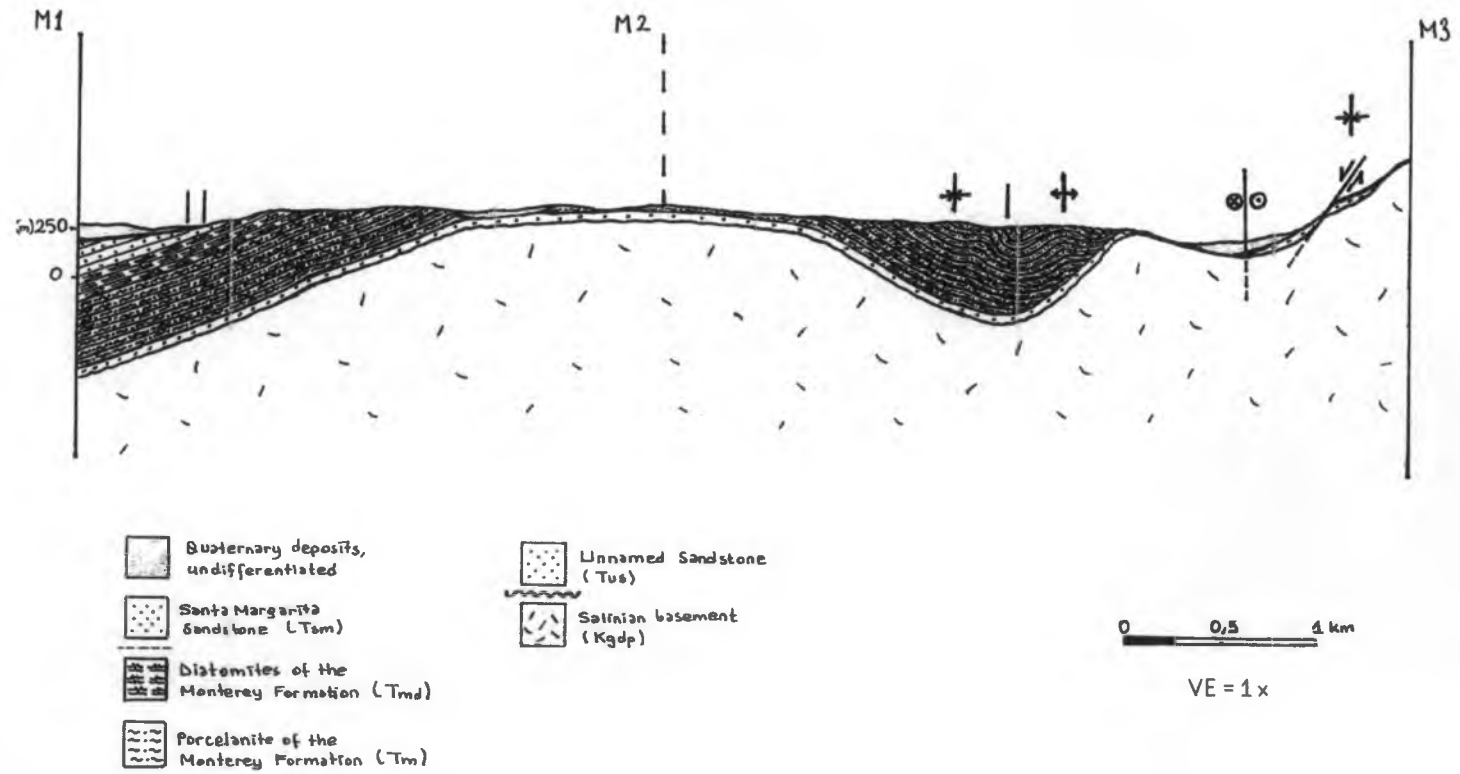


Figure 33. North-southwest cross section M1—M3, along Toro Road to the south (see Figure 26 for location).



Figure 34. Diatomite exposure on the Toro Road, Monterey area.



Figure 35. Diatomite sample, 1.1, collected from along Toro Road, Monterey area (Table 3).

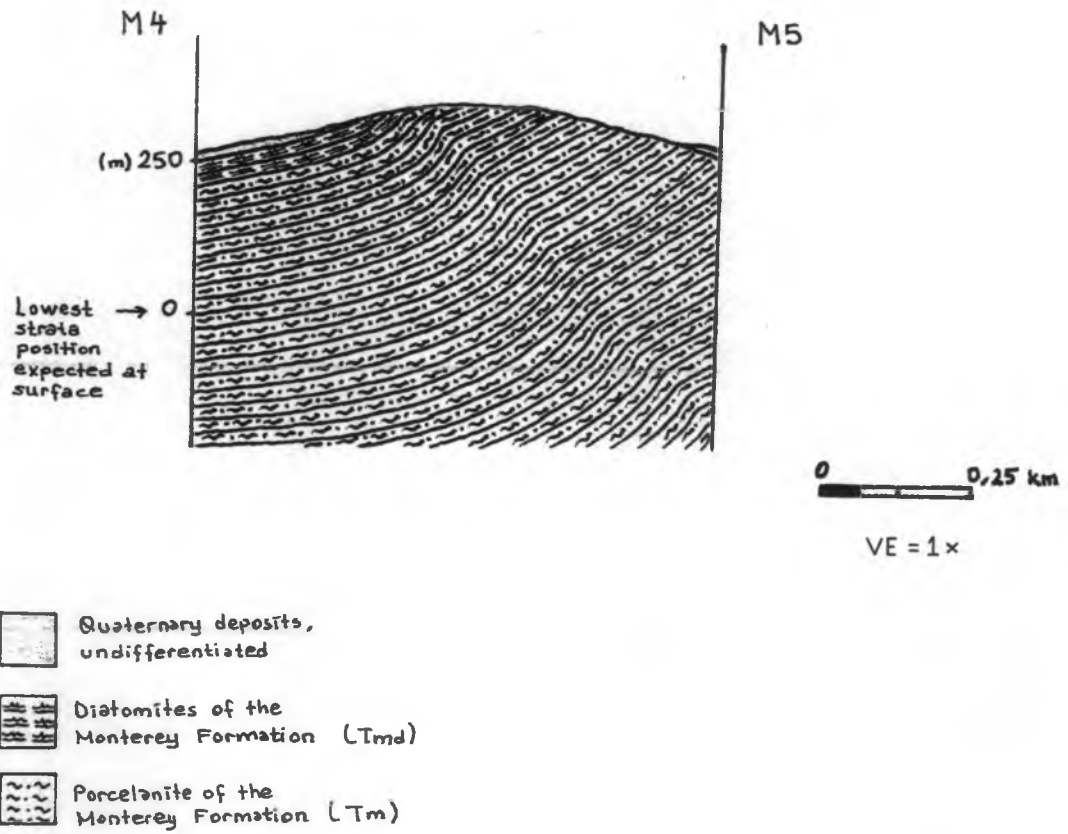


Figure 36. Northwest-southeast cross section M4—M5, west of Toro Road (see Figure 26 for location)

Table 7. Estimated minimum thicknesses of the lithologic units in my cross sections in the Monterey area.

Lithologic unit	Estimated thickness (m)	Clark's estimations (1984) (m)
Santa Margarita sandstone (Tsm)	148	150
Diatomite of Monterey (Tmd)	40 to 120	250
Porcelanite of Monterey (Tm)	288 to 385	600
Siliceous mudstone of Monterey (Tml)	87	30
Unnamed sandstone (Tus)	12 to 34	60

4.3.2. Petrographic Analysis of Silica on Monterey Formation

I did petrographic analysis of five thin sections from the sampling locations in the Monterey area; the samples include 8.5, 6.1, 15.4, 4.1 and 1.1 (Table 3). I used the same methods described previously for the Pt Reyes samples

Sample 8.1.T is rich in detrital quartz, and feldspar grains, and no carbonate is present. It has nearly %25-35 biogenic silica, and there are no fossils visible. 6.1, 4.1, and 15.4 have approximately %50 biogenic silica and detrital quartz.

Sample 1.1 is a diatomite, but diatomite fragments were not visible. The reason could be that diatomite frustules and quartz may sometimes stick together, and the tools I used, polarizing and reflected light microscopes, do not isolate diatoms, and they do not clearly show up. Even though petrographic analysis is not a good method to view diatom shells and hand specimen characteristics, the broad hump in XRD that characterizes opal-A presence allowed me to be confident that the sample is composed of diatomaceous material.

SYSTEM	SERIES	TORO ROAD - MONTEREY COAST - NORTH OF POTRERO CANYON				
		Formation	Lithology	Thickness (m)	Lithology Description	
TERTIARY	MIOCENE	MONTEREY FORMATION	Santa Margarita sandstone (Tsm)		145	Thick-bedded white to gray coarse- to fine-grained arkosic sandstone
			Tmd		40 to 120	Thick-bedded white diatomite with thin brownish chert lenses and thick grayish pumicite interbeds
				Tm		215 to 485
			Tml			80
			Unnamed sandstone (Tus)		14 to 30	Thick-bedded medium- to fine grained arkosic sandstone
		CRETACEOUS and OLIGOCENE		Salinian basement rocks (KgdP)		

Figure 37. Stratigraphic column of along Toro Road, north of Potrero Canyon and Monterey coast, Monterey area.

4.3.3. X-Ray Mineralogy of Silica on Monterey Formation

I ran eleven samples of the Monterey Formation in the Monterey area (Table 3). I followed the same qualitative method used for the sample set from Point Reyes area; I distinguished major silica phases and the peaks of biogenic quartz from detrital quartz by comparing peak values in the XRD patterns of my samples with the ones shown in Figures 8 and 9.

Samples 8.5, 8.12, and 9.1, are estimated to be composed of approximately %30 biogenic silica, and %70 detrital constituents, largely clay minerals, and small amount of Tridymite and Calcite. The samples have a distinctive quartz signal as the major silica phase (Appendices F.1, F.2 and F.3). These three samples are similar to samples, 8.1.T, and 8.6, from Point Reyes based on my hand specimens, field observations, petrographic analysis, and Kelham and Isaacs's diagram (1985) (Figure 6).

Samples 11.1 and 11.5 have opal-CT as a major silica phase indicating nearly %30 biogenic silica, and a couple of sharp quartz peaks indicating some detrital quartz. They also have high content of clay and small amount of calcite. (Appendices G.1, and G.2).

Samples 6.1, 15.4, 3.2, and 4.1 have opal-CT as a major silica phase of nearly %50 biogenic silica, and a couple of sharp detrital quartz peaks and one broad opal-A hump at 26° , 2θ . They are also rich in clay (Appendices H.1, H.2, I.1 and I.2).

1.1 has intermediate pattern of opal-A and opal-CT. It has a couple of sharp detrital quartz peaks, and considerable amount of clay (Appendix J.1).

Finally sample 16.2 has quite a different pattern from the other samples'. Even though the pattern looks very similar to the quartz pattern, they do not match with the

sharpest quartz peaks, and clay minerals are the only ones matching the small peaks. I collected this sample from the area having diatomites along Toro Road, and I can suggest that this sample is most likely coming from a detritus-rich part in the section (Appendix K.1). Overall the major silica phases of my samples are shown in Table 8 and Figure 38.

Table 8. XRD results of the Monterey Formation samples in the Monterey area

Sample ID	Lithology	Major silica phase
8.5	siliceous mudstone	quartz
8.12	siliceous mudstone	quartz
9.1	siliceous mudstone	quartz
11.1	siliceous mudstone	opal-CT
11.5	siliceous mudstone	opal-CT
6.1	porcelanite	opal-CT
15.4	porcelanite	opal-CT
3.2	diatomaceous porcelanite	opal-CT
4.1	diatomaceous porcelanite	opal-CT
1.1	diatomite	opal-A + opal-CT
16.2	diatomite	detrital

4.4. Diagenetic History of the Monterey Formation in the Monterey Area

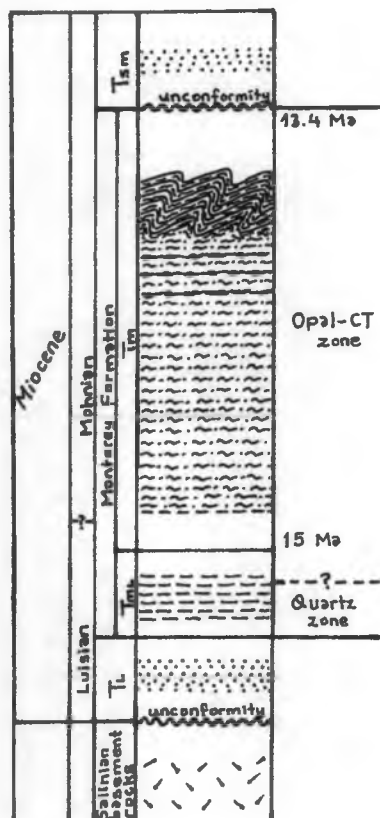
The lower member of the Monterey Formation around Whispering Pines Park and Carmel Woods in the Monterey area include both opal-CT and quartz phase biogenic silica. Three samples, 8.5, 8.12, 9.1, have been buried deeper than another two samples, 11.1, 11.5, based on superposition. These three more deeply buried samples contain approximately %30 biogenic quartz since there is no opal-A or opal-CT signal in the

XRD pattern. This supports my contention that this siliceous mudstone section has been buried deeper, reaching the depths required to transform opal-CT to biogenic quartz (Table 8). When we look at the diffraction patterns of the other two samples, 11.1, 11.5, opal-CT appears to be the major silica phase. This suggests that they have not been buried deep enough to convert opal-CT to quartz. However, they must have almost reached the burial depth required for opal-CT to quartz transformation since they are the upper part of the nearly 87-m-thick siliceous mudstone section (Table 7).

The middle porcelanite member around Pacific Meadows Park, Boots and Saddle Road and Laureles Grade in the area are composed of opal-CT as the major biogenic silica phase. It suggests that the approximately 288 to 385 m-thick middle section has not been buried deep enough to convert opal CT to quartz.

The youngest Monterey member exposed in the study area is mostly made of diatomite and diatomaceous shale; it reveals an intermediate pattern between opal-A and opal-CT in XRD analysis, and is transitional to the underlying porcelanite member. The approximately 40 to 120 m-thick diatomite section in the region must have been heated to nearly $\sim 42^{\circ}\text{C}$ (Figure 6) to reach the opal-A to opal-CT transition zone. Major silica phases of Monterey members between Monterey and Point Reyes areas are shown in Figure 38.

Sculptured Beach - Kehoe Beach and
North of Drakes Bay



Toro Road - Monterey Coast and
North of Potrero Canyon

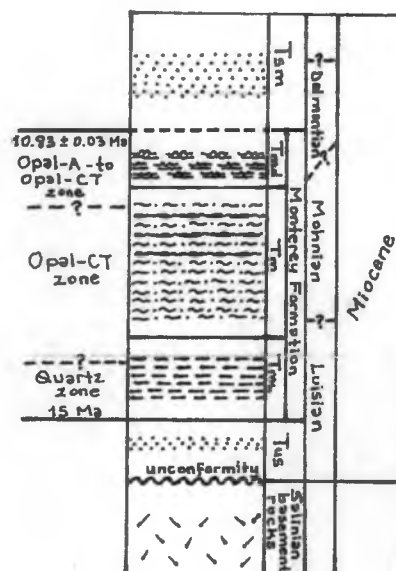


Figure 38. Stratigraphic and diagenetic comparison of the Monterey sub members between Point Reyes and Monterey areas.

4.4.1. Estimated Burial Depths of the Monterey Formation

Like the Point Reyes calculations, I used the range of present-day geothermal gradient of 25°C to 50°C (MacKinnon, 1989; Brink et al., 2000), and a high geothermal

gradient of 55°C, as two different scenarios. I again assumed that the surface temperature was 15°C, and entire section was diatomaceous. This time, I used Clark thickness estimation since my estimations for the thickness of the middle porcelanite member of the Monterey Formation in the Monterey area is unconstrained by my cross sections (Figures 30 and 36).

Table 9. Calculations showing the ranges of minimum burial depths of the Monterey Formation members, Point Reyes. Minimum estimated thicknesses were provided from Clark et al. (1984), and the minimum burial temperatures are from Figure 6.

Surface temp. (°C)	Thermal gradient (°C/km)	Monterey members	Min. estimated thicknesses (m)	Min. burial temp. (°C)	Estimated burial depths (m)	Min. burial depths (m)
15	25	Diatomite	250	43	1120	2000
		Porcelanite + Siliceous mudstone	630	65	2000	
	50	Diatomite	250	43	560	1190
		Porcelanite + Siliceous mudstone	630	65	1000	
	55	Diatomite	250	43	509	1139
		Porcelanite + Siliceous mudstone	630	65	909	

My estimations of the range of minimum burial depth is 1139 to 2000 m., and the range of minimum amount of overburden is 259 to 1120 m. required for the diagenesis of the entire Monterey Formation in the Monterey area.

5.0. Discussion

This study enabled us to better characterize the stratigraphic and diagenetic characteristics of the Monterey Formation in the Point Reyes and Monterey areas. The differences in the estimated minimum thicknesses of the Monterey Formation members between two areas are some of the most significant results of this work. It reveals quite different depositional histories of the Monterey Formation in the two study areas. The thicker and more siliceous section of Monterey Formation in the Point Reyes area contrasts with the section in Monterey area and indicates that the Monterey Formation in the Point Reyes area accumulated in the closer to the center of is the Bodega Basin and further offshore while the Monterey area section likely accumulated closer the margin of the basin in proximity to land. As a consequence of having different depositional histories, the Monterey Formation in these areas experienced different overburden pressure resulting in dissimilar burial histories for the Monterey Formation in the Point Reyes and Monterey areas. Additionally, the Monterey Formation at Point Reyes may have experienced a higher geothermal gradient during the timing of its deposition and this may have resulted in a more diagenetically altered younger chert section. This contrasts with the diatomites of the Monterey Formation in the Monterey area that underwent late diagenesis but are, overall, less diagenetically altered due to less overburden pressure. Thus, this study suggests that the Monterey Formation of Point Reyes was a thicker section and was more diagenetically altered (pre-erosion) than the Monterey Formation in the Monterey area.

Comparing my findings of the Monterey Formation in northern California with the previous studies of the Monterey Formation in southern California indicates that the Monterey Formation in my two study locations are not as oil-bearing as the Monterey Formation in southern California. Although the Monterey Formation in the Point Reyes area experienced more diagenetic alteration than in the Monterey area sections, it did not reach enough burial depth to initiate the kerogen maturation. When we consider the burial depths the Monterey Formation reached in relatively broader and bigger basins in southern California, it is not surprising that the Monterey Formation of northern California is not as productive as the Monterey Formation of southern coast.

Overall, the stratigraphic and diagenetic characteristics of the Monterey Formation in the two areas of study suggest that the Monterey Formation has a slightly different geological history in the Point Reyes and Monterey areas. As a consequence of that different history, the Monterey Formation in the Point Reyes area is thicker, more siliceous, and underwent diagenesis earlier than the Monterey Formation in the Monterey area. However, both of the Monterey Formation sections in the two study areas were not thick enough or buried deep enough to initiate the kerogen maturation. Overall, this information provides further insights into the timing of petroleum generation and why these basins in northern California are less productive. In the concluding sections of my thesis I outline the significance of distinctive depositional and burial histories of the Monterey Formation along the California coast and the relationship to petroleum potential.

6.0. Conclusions

6.1. Stratigraphic Comparison of the Monterey Formation, Point Reyes and Monterey Areas

The Monterey Formation today exposed at Point Reyes and Monterey area, may have been almost contiguous at the time of deposition. Therefore they may have experienced similar deformation histories and high heat flow during the timing of diagenesis.

It appears that the lower siliceous mudstone and middle porcelanite members in both area are stratigraphically and diagenetically correlative based on lithologic and diagenetic similarities. However, the diatomaceous sediment in the Monterey area is younger and is in the opal-A to opal-CT transformation zone, and it is most likely not correlative with any member exposed at Point Reyes.

My estimations of the minimum thickness of the lithologic units based on the cross- sections I built and Clark et al. (1984) data suggest that the entire Monterey Formation at Point Reyes is thicker than the Monterey Formation in the Monterey area. The reason may be that the Point Reyes area was likely close to the center and deeper part of the basin where there was more accommodation allowing thicker sedimentation, while the Monterey area was closer to the margin of the basin where accommodation space was more limited.

I can also suggest that the middle part of the Monterey Formation at Point Reyes is more siliceous than the middle part of the Monterey in the Monterey area. One possible explanation is that the Point Reyes area was further offshore while the Monterey area was closer to land. In this scenario, the Pt Reyes section received more organic rich, siliceous

sediments from the marine environment while the Monterey in the Monterey area received more detrital sediments from the nearby landmass

6.2. Diagenetic Comparison of the Monterey Formation, Point Reyes and Monterey Areas

The minimum burial depth and the amount of erosion calculations I made suggest that the Monterey Formation was buried at least 1138 to 2000 m around the Santa Cruz area before Santa Margarita sandstone deposition, resulting in opal-A to opal-CT transformation in the upper member exposed at Sculptured Beach, and opal-CT to quartz transformation in the lower siliceous mudstone member exposed at Kehoe Beach. The rocks then underwent a rapid uplift and erosion. I infer approximately 391 to 283 m. of erosion occurring during the transportation of the rocks along the SGFZ. Then, glauconites of the basal Santa Margarita Sandstone were deposited on top of highly contorted opal-CT chert.

For the Monterey area, my findings require 1139 to 2000 m. of the minimum burial depth and 259 to 1120 m. overburden pressure coming from post-Monterey Formation strata. In contrast to the Point Reyes area, there is no unconformity between the Monterey Formation and overlying sandstone in the Monterey area suggesting that there has not been erosion of the Monterey rocks. Therefore, diagenesis most likely occurred later than Santa Margarita sandstone deposition, and the rest of the overburden pressure required for the diagenesis was provided by post-Monterey Formation rocks since there has never been enough overlying Monterey rocks to cause the diagenesis.

6.3 Comparison of the Petroleum Potential of the Monterey Formation between northern and southern California

The Monterey Formation in the Point Reyes and Monterey area is not an efficient petroleum source like the Monterey Formation of southern California. Reasons include differences in the shape of the coastline, water current and amount of sunlight, factors that control the intensity of oceanic upwelling. Upwelling increases diatom productivity and the amount of organic matter preserved. It appears as if upwelling was more intense in Southern California, resulting in better preservation of organic matter compared to the northern coast.

Depth of burial is another key factor. As the consequence of difference in intensity of oceanic upwelling, the Monterey Formation in southern California is thick and has been buried nearly 3 to 6 km. In comparison, the Monterey Formation at Point Reyes and the Monterey area has been buried only 1.1 to 2 km, which not enough to generate significant hydrocarbons.

7.0 References

- Atwater, T., 1970, Implications of Plate Tectonics for the Cenozoic Tectonic Evolution of Western North America: *Geological Society of America Bulletin*, v. 81, p. 3513–3536.
- Atwater, T., and Stock, J., 1998, Pacific-North America Plate Tectonics of the Neogene Southwestern United States: An Update: *International Geology Review*, v. 40, p. 375–402.
- Behl, R.J., 1992, Chertification in the Monterey Formation of California and deep-sea sediments of the West Pacific: University of California, Santa Cruz.
- Behl, R.J., 1999, Since Bramlette (1946): The Miocene Monterey Formation of California revisited: *Geological Society of America Special Papers*, v. 338, p. 301–313.
- Behl, R.J., and Smith, B.M., 1992, Silicification of deep-sea sediments and the oxygen isotope composition of diagenetic siliceous rocks from the western Pacific, Pigafetta and east Mariana basins, Leg 129: *Proc. ODP, Sci. Results*, v. 129, p. 81–117.
- Biddle, K.T., 1991, The Los Angeles Basin: An Overview: Chapter 1: v. 135, p. 5–24.
- Blake, J.R., Jayko, M.C., and Howell, D., 1981, Geology of a Subduction Complex in the Franciscan Assemblage of Northern California: *Oceanologica Acta*, Special issue.
- Brown, E.H., 1962. Geology of the Rancho San Carlos area, Monterey County.
- Bowen, O.E., 1965, Stratigraphy, Structure, and Oil Possibilities in Monterey and Salinas Quadrangles, California: ABSTRACT: *AAPG Bulletin*, v. 49, p. 1081–1081.
- Bowen, O.E., and Gray, C.H., 1959, Geology and economic possibilities of the limestone and dolomite deposits of the northern Gabilan Range, California: San Francisco, California. Division of Mines and Geology. Special report 56, 40 p.
- Brabb, E.E., 1989, Geologic map of Santa Cruz County, California: *IMAP USGS Numbered Series* 1905.
- Calvert, S.E., 1966, Origin of Diatom-Rich, Varved Sediments from the Gulf of California: *The Journal of Geology*, v. 74, p. 546–565.

Clark, J.C., 1981, Stratigraphy, paleontology, and geology of the central Santa Cruz Mountains. California Coast Ranges: U.S. Geological Survey Professional Paper 1168, 51 p.

Clark, J.C. and Brabb, E.E., 1978. Stratigraphic contrasts across the San Gregorio fault, Santa Cruz Mountains, west central California. Calif. Div. Mines and Geol. Special Report, 137, pp.3-12.

Clark, J.C., and Brabb, E.E., 1997, Geology of Point Reyes National Seashore and vicinity, California: a digital database: U.S. Geological Survey, Open-File Report USGS Numbered Series 97-456.

Clark, J.C., Brabb, E.E., Greene, H.G., and Ross, D.C., 1984, Geology of Point Reyes Peninsula and Implications for San Gregorio Fault History: p. 67–85.

Clark, J.C., Brabb, E.E., MacKinnon, T., Gilbert, J.R., and Northern California Geological Society, 2003, Geology of the Point Reyes area, California: Saturday, September 27, 2003 : trip leader, Tom MacKinnon ; co-leader, John R. (Rusty) Gilbert: [California], Northern California Geological Society.

Clark, J. C., Dupre, William R., and Rosenberg, Lewis I., 1997, Geologic Map of the Monterey and Seaside 7.5-minute Quadrangles, Monterey County, California: A Digital Database: U.S. Geological Survey Open-File Report 97-30.

Clague, J. J., 1969, Landslides of southern Point Reyes National Seashore: California Div. Mines and Geology Mineral Inf. Service, v. 22, p. 107-110, 116-118.

Crouch, J.K., and Suppe, J., 1993, Late Cenozoic tectonic evolution of the Los Angeles basin and inner California borderland: A model for core complex-like crustal extension: Geological Society of America Bulletin, v. 105, p. 1415–1434.

Dickinson, W.R., and Geological Society of America, 2005, Net dextral slip, Neogene San Gregorio-Hosgri fault zone, coastal California geologic evidence and tectonic implications: Boulder Colo., Geological Society of America.

Dunkel, C.A., and Piper, K.A., 1997, 1995 National assessment of United States oil and gas resources: Assessment of the Pacific Outer Continental Shelf Region: U.S. Department of the Interior Minerals Management Service MMS 97-0019, 207 p.

Dupre, W.R., 1990, Quaternary Geology of the Monterey Bay Region, California: p. 185–191.

Fairbanks, H.W., 1903, Description of the San Luis Quadrangle.

Fiedler, W.M., 1944, Geologic map of the Jamesburg Quadrangle, Monterey County, California.

Galloway, A.J., 1977, Geology of the Point Reyes Peninsula, Marin County, California: California Division of Mines and Geology, 202.

Graham, S.A., 1976, Tertiary sedimentary tectonics of the central Salinian block of California.

Graham, S.A., and Williams, L.A., 1985, Tectonic, Depositional, and Diagenetic History of Monterey Formation (Miocene), Central San Joaquin Basin, California: AAPG Bulletin, v. 69, p. 385–411.

Greene, H.G., Lee, W.H.K., McCulloch, D.S., and Brabb, E.E., 1973, Faults and earthquakes in the Monterey Bay region, California: Miscellaneous Field Studies Map USGS Numbered Series 518.

Greene, H.G., 1990, Regional tectonics and structural evolution of the Monterey Bay region, central California, *in* Garrison, R.E., Greene, H.G., Hicks, K.R., Weber, G.E., and Wright, T.L., eds., Geology and tectonics of the central California coast region, San Francisco to Monterey: Pacific Section, American Association of Petroleum Geologists, Book GB67, p. 31–56.

Grove, K., and Stozek, B., 2013, Geophysical and sedimentologic evidence for Plio-Pleistocene deformation in the offshore San Andreas fault zone between Gualala and San Francisco, Northern California: Abstracts with Programs - Geological Society of America, v. 45, p. 16–17.

Herold, C.L., 1934, Fossil Markings in the Carmelo Series (Upper Cretaceous [?]), Point Lobos, California: The Journal of Geology, v. 42, p. 630–640.

Hornafius, J.S., 1985, Neogene tectonic rotation of the Santa Ynez Range, Western Transverse Ranges, California, Suggested by paleomagnetic investigation of the

Monterey Formation: *Journal of Geophysical Research: Solid Earth*, v. 90, p. 12503–12522.

Howell, D.G., Vedder, J.G., and McDougall, K., 1977, Frontmatter: *Cretaceous Geology of the California Coast Ranges, West of the San Andreas Fault*: p. i–vii.

Ingle Jr, J.C., 1980. Cenozoic paleobathymetry and depositional history of selected sequences within the southern California continental borderland. Cushman Foundation for Foraminiferal Research Special Publication, 19, pp.163-195.

Isaacs, C.M., 1984, *Geology and Physical Properties of the Monterey Formation, California*, in *Society of Petroleum Engineers*.

Isaacs, C.M., 1981, Porosity Reduction During Diagenesis of Monterey Formation, Santa Barbara, California: ABSTRACT: AAPG Bulletin, v. 65, p. 940–941.

Isaacs, C.M., Baumgartner, T.R., Tennyson, M.E., Piper, D.Z., and Ingle, J.C., 1996, A prograding margin model for the Monterey Formation, California, American Association of Petroleum Geologists and Pacific Section SEPM (Society of Sedimentary Geology) Annual Meeting Abstracts, V. 5, p. 69.

Isaacs, C.M. (Geological S., and Baumgartner, T.R. (Scripps I. of O., 1996, A Prograding Margin Model for the Monterey Formation, California: AAPG Bulletin, v. 5.

Isaacs, C.M., and Rullkötter, J., 2001, *The Monterey Formation: From Rocks to Molecules*: Columbia University Press, 563 p.

Jarvie, D.M., and Lundell, L.L., 2001, Kerogen type and thermal transformation of organic matter in the Miocene Monterey Formation, in *United States*, Columbia University Press : New York, NY, United States, p. 268–295.

Keller, M.A., and Isaacs, C.M., 1985, An evaluation of temperature scales for silica diagenesis in diatomaceous sequences including a new approach based on the Miocene Monterey Formation, California: *Geo-Marine Letters*, v. 5, p. 5.

Lagoë, M.B., 1987, The Stratigraphic Record of Sea-Level and Climatic Fluctuations in an Active-Margin Basin: The Stevens Sandstone, Coles Levee Area, California: *PALAIOS*, v. 2, p. 48–68.

Lawson, A.C., and Posada, J. de la C., 1893, *The geology of Carmelo Bay*: Berkeley, The University.

Lee, D.R. Characterisation and the diagenetic transformation of non- and micro-crystalline silica minerals.

Leinen, M., 1977, A normative calculation technique for determining opal in deep-sea sediments: *Geochimica et Cosmochimica Acta*, v. 41, p. 671–676.

Littke, R., Fourtanier, E., Thurow, J.W., and Taylor, E., 1991, Composition and distribution of silica in sediments of the Broken Ridge.

MacKinnon, T.C. (Ed.), 1989, *Oil in the California Monterey Formation: Los Angeles to Santa Maria, California, July 20 - 24, 1989*: Washington, DC, American Geophysical Union, Field trip guidebook 28th International Geological Congress ; 311, 55 p.

Mata, S.A., Corsetti, C.L., Corsetti, F.A., Awramik, S.M., and Bottjer, D.J., 2012, Lower cambrian anemone burrows from the upper member of the wood canyon formation, death valley region, united states: paleoecological and paleoenvironmental significance: *PALAIOS*, v. 27, p. 594–606.

Mayerson, Drew. 1997. Santa Maria-Partington Basin, in Dunkle, C and Piper, K. eds, 1995 National Assessment of United States Oil and Gas Resources — Assessment of the Pacific Outer Continental Shelf Region: Minerals Management Service OCS Report 97-0019, pp. 84-95.

McCulloch, D.S. and Greene, H.G., 1989. Geologic map of the central California continental margin. California Continental Margin Geologic Map Series, central California continental margin, map A, 5.

McDougall, K., 1987, Foraminiferal Biostratigraphy and Paleoecology of Marine Deposits, Goler Formation, California, p. 43–67.

McDougall, K.A., 1994, Late Cenozoic benthic foraminifers of the HLA borehole series, Beaufort Sea shelf, Alaska: U.S. G.P.O. ; For sale by U.S. Geological Survey, Map Distribution, Bulletin USGS Numbered Series 2055.

McLaughlin, R.J., Sliter, W.V., Sorg, D.H., Russell, P.C., and Sarna-Wojcicki, A.M., 1996, Large-scale right-slip displacement on the East San Francisco Bay Region fault

system, California: Implications for location of late Miocene to Pliocene Pacific plate boundary: *Tectonics*, v. 15, p. 1–18.

Murata, K.J. and M.B. Norman 1976. An index of crystallinity for quartz. *American Journal of Science*, v. 276, p. 1120-1130, 2010, *GeoArabia, Journal of the Middle East Petroleum Geosciences*, v. 0.

Nicholson, C., Sorlien, C.C., Atwater, T., Crowell, J.C., and Luyendyk, B.P., 1994, Microplate capture, rotation of the western Transverse Ranges, and initiation of the San Andreas transform as a low-angle fault system: *Geology*, v. 22, p. 491–495.

O'Rourke, J.T., 1980, Geotechnical Investigation, Carmel Valley Ranch, Monterey County, California: Department of Applied Earth Sciences, Stanford University, 132 p.

Pisciotta, K.A., and Garrison, R.E., 1981, Lithofacies and Depositional Environments of the Monterey Formation, California: p. 97–122.

Richard G. Stanley, P.G.L., 2000, Oil-bearing rocks of the Davenport and Point Reyes areas and their implications for offset along the San Gregorio and northern San Andreas faults: *Stanford University Publication Geological Sciences*, v. 21, p. 371–384.

Rosenberg, L., 1993, Earthquake and landslide hazards in the Carmel Valley area, Monterey County, California.

Rosenberg, L.I., Clark, J.C., 1994. "Quaternary faulting of the Greater Monterey Area, California: Final Technical Report as part of the National Earthquake Hazards Reduction Program, Program Element II, Component II". 5, 28 p.

Rubey, W.W., 1981, *The Geotectonic development of California*: Prentice Hall PTR, 734 p.

Rullkoetter, J., and Isaacs, C.M., 1996, *Monterey Source Rock Facies and Petroleum Formation - a Synthesis of Results of the Cooperative Monterey Organic Geochemistry Study*.

Stoffer, P.W. 2005. *Geology at Point Reyes National Seashore and Vicinity, California: A Guide to San Andreas Fault Zone and the Point Reyes Peninsula*. In *The San Andreas Fault and the San Francisco Bay Area, California: A Geology Fieldtrip Guidebook to Selected Stops on Public Lands*. U.S. Geological Survey Open File Report 2005-1127.

Stozek, B.A., 2012, Geophysical evidence for quaternary deformation within the offshore San Andreas Fault System, Northern California [Thesis]: San Francisco State University.

Taliaferro, N.L., 1933, *The Relation of Volcanism to Diatomaceous and Associated Siliceous Sediments*, by N. L. Taliaferro: University of California press, 55 p.

Ten Brink, U.S., Zhang, J., Brocher, T.M., Okaya, D.A., Klitgord, K.D., and Fuis, G.S., 2000, Geophysical evidence for the evolution of the California Inner Continental Borderland as a metamorphic core complex: *Journal of Geophysical Research: Solid Earth*, v. 105, p. 5835–5857.

Titus, S.J., Crump, S., McGuire, Z., Horsman, E., and Housen, B., 2011, Using vertical axis rotations to characterize off-fault deformation across the San Andreas fault system, central California: *Geology*, v. 39, p. 711–714.

Tolman, C.F., 1927, Biogenesis of hydrocarbons by diatoms: *Economic Geology*, v. 22, p. 454–474.

Weaver, C.E., 1949a, *Geology of the Coast Ranges Immediately North of the San Francisco Bay Region, California*: Geological Society of America Memoirs, v. 35, p. 1–229.

Weaver, C.E., 1949b, *Geology of the Coast Ranges Immediately North of the San Francisco Bay Region, California*: Geological Society of America Memoirs, v. 35, p. 1–229.

White, L.D., 1992, Chapter I - Overview of the Monterey Formation: Dating Techniques, Sedimentary Components, and Paleooceanographic Parameters, p. 3–5.

White, L.D., 1989, *Chronostratigraphic and paleooceanographic aspects of selected chert intervals in the Miocene Monterey Formation, California*: University of California, Santa Cruz, 540 p.

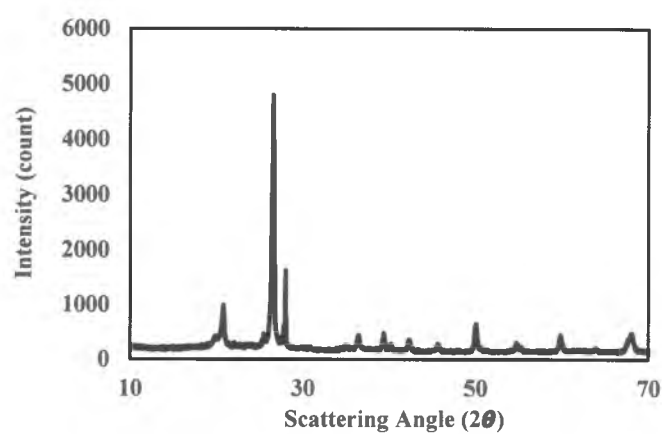
White, L.D., Garrison, R.E., and Barron, J.A., 1992, Miocene intensification of upwelling along the California margin as recorded in siliceous facies of the Monterey Formation and offshore DSDP sites: Geological Society, London, Special Publications, v. 64, p. 429–442.

Wright, T.L., Greene, H.G., Hicks, K.R., and Weber, G.E., 1990, AAPG June 1990 field trip road log, coastal geology-San Francisco to Monterey, in Garrison, R.E., Greene, H.G., Hicks, K.R., Weber, G.E., and Wright, T.L., eds., *Geology and tectonics of the central California coastal region, San Francisco to Monterey: American Association of Petroleum Geologists, Volume and Guidebook, Pacific Section, Bakersfield, Calif.*, p. 261-314.

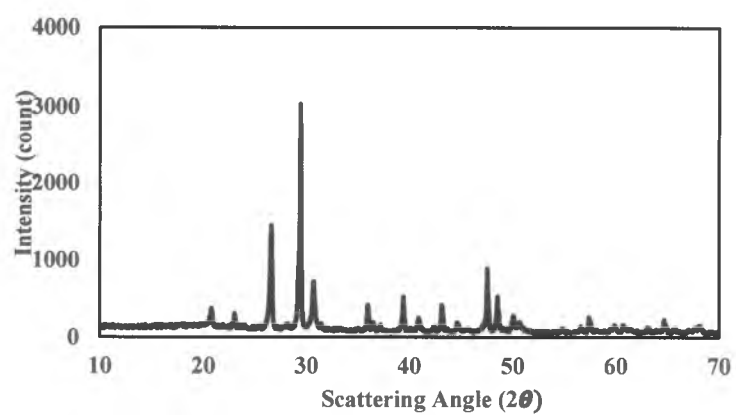
8.0 Appendices

A. XRD signals of quartz siliceous mudstone samples in the Point Reyes 8area

1. Sample 8.1.T, Kehoe Beach

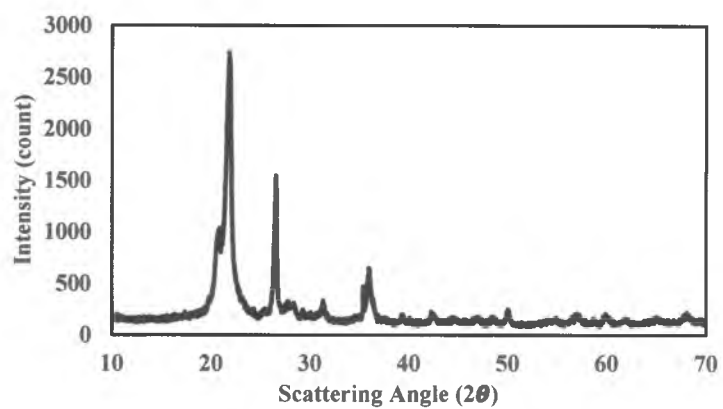


2. Sample 8.6, Kehoe Beach

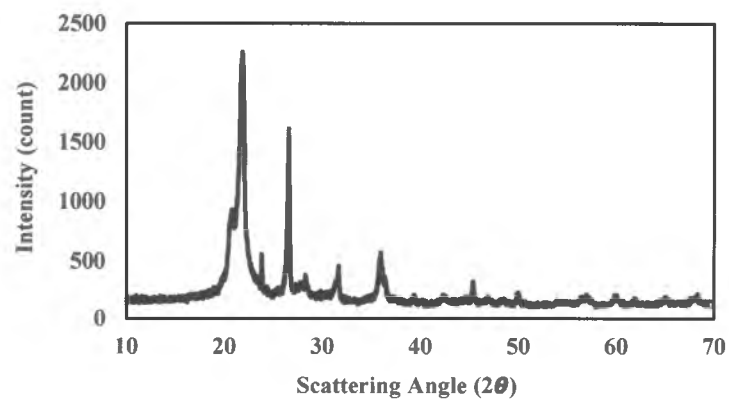


B. XRD signals of opal-CT siliceous mudstone samples in the Point Reyes area

1. Sample 8.1.T.1, Kehoe Beach

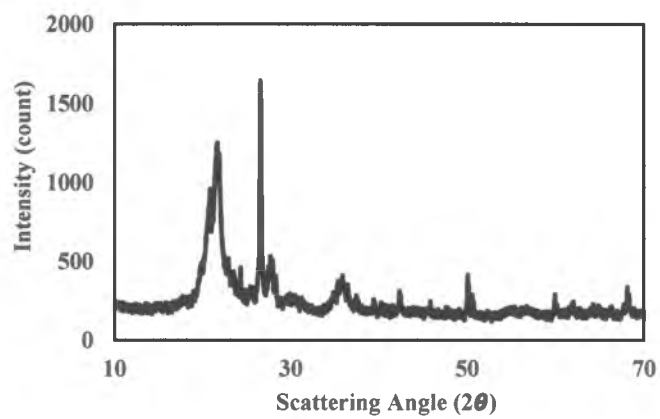


2. Sample 8.1.T.2, Kehoe Beach

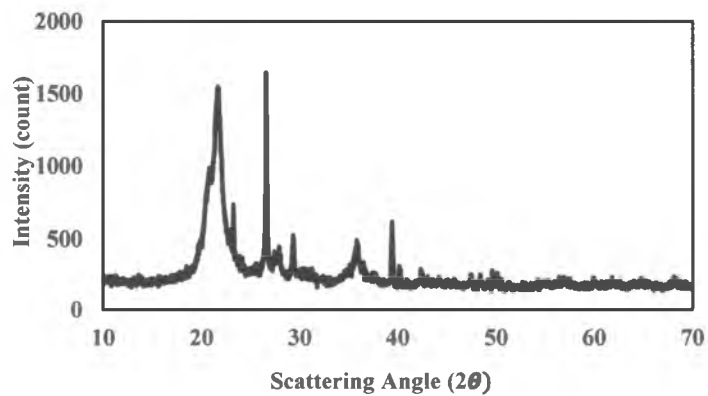


C. XRD signals of opal-CT porcelanite samples in the Point Reyes area

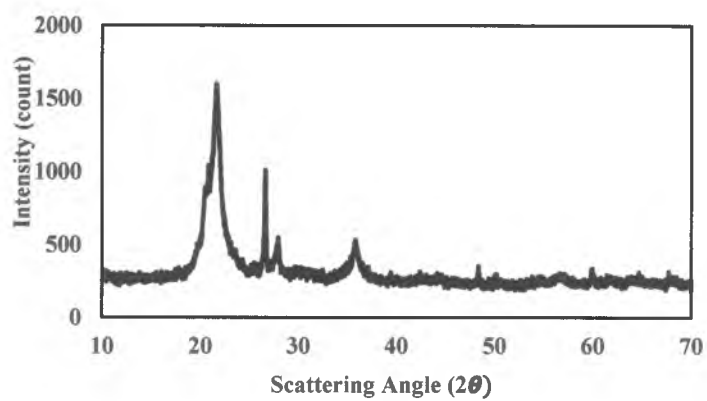
1. Sample 9.5, NW of Drakes Bay



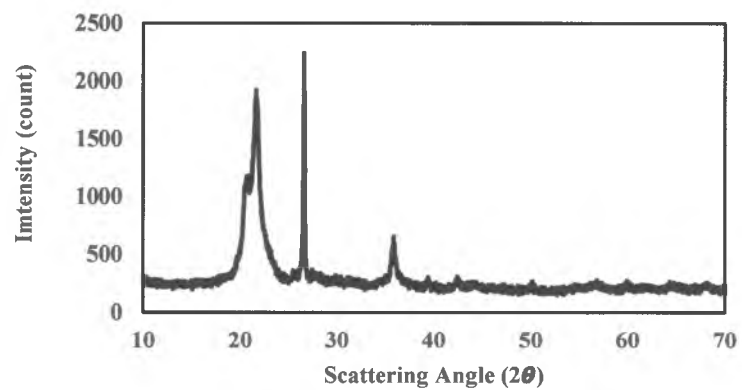
2. Sample 7.1, NW of Drakes Bay



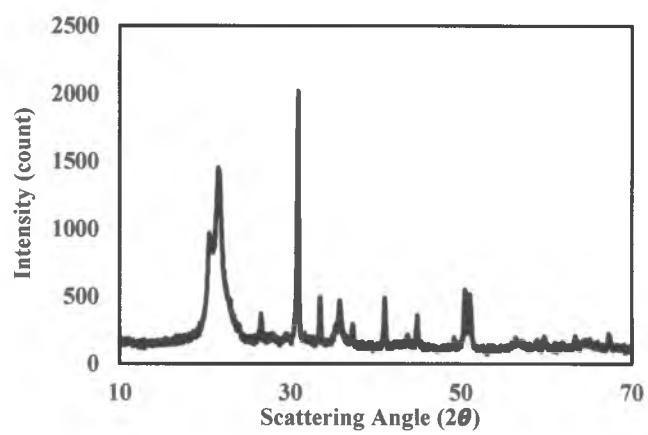
3. Sample 6.1, NW of Drakes Estero



4. Sample 3.1, NW of Drakes Estero

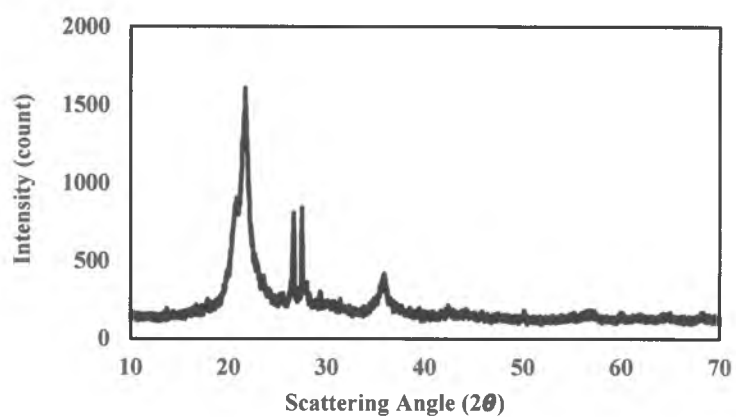


5. Sample 9.2, Sculptured Beach

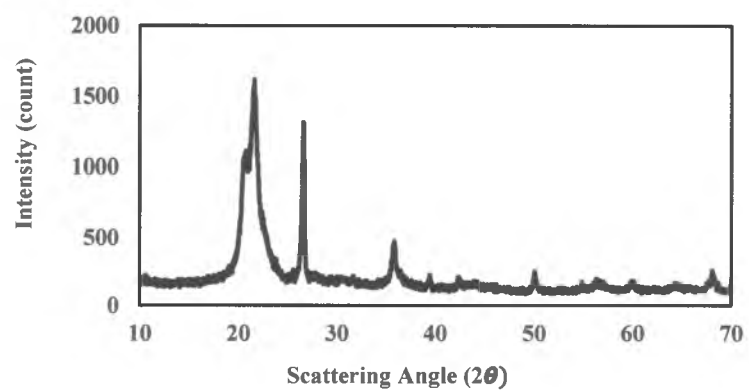


D. XRD signals of opal-CT chert samples in the Point Reyes area

1. Sample 9.4, N of Sculptured Beach

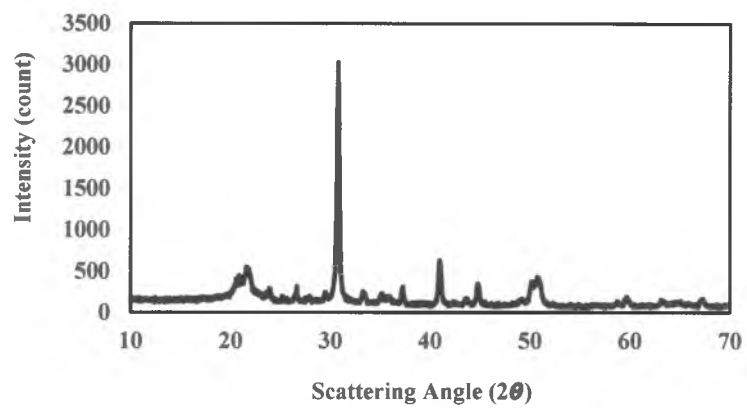


2. Sample 9.3, Sculptured Beach



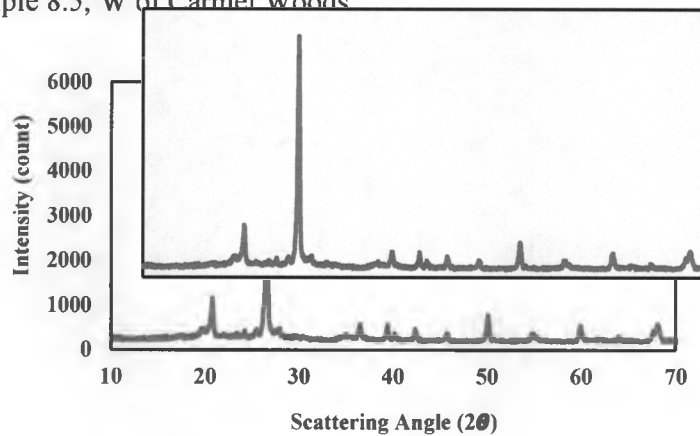
E. XRD signals of dolomite rich porcelanite in the Point Reyes area

1. Sample 9.1, Sculptured Beach

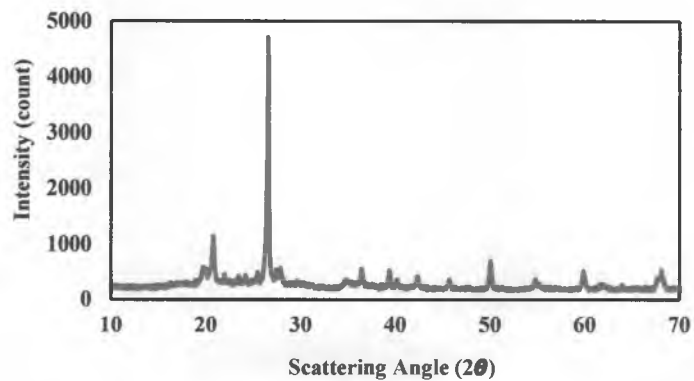


F. XRD signals of quartz siliceous mudstone samples in the Monterey area

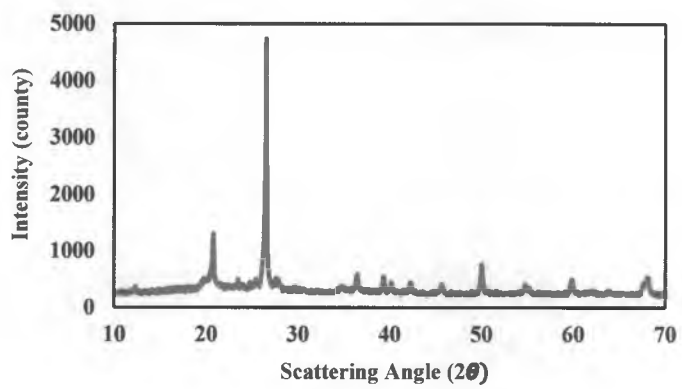
1. Sample 8.5, W of Carmel Woods



2. Sample 8.12, SW of Carmel Woods

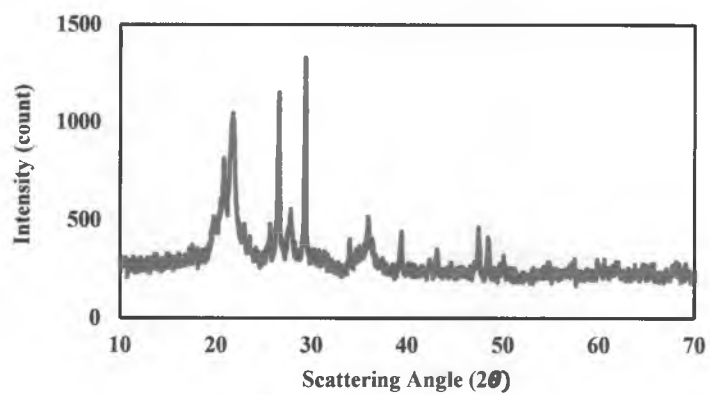


3. Sample 9.1, SW of Whispering Pines Park

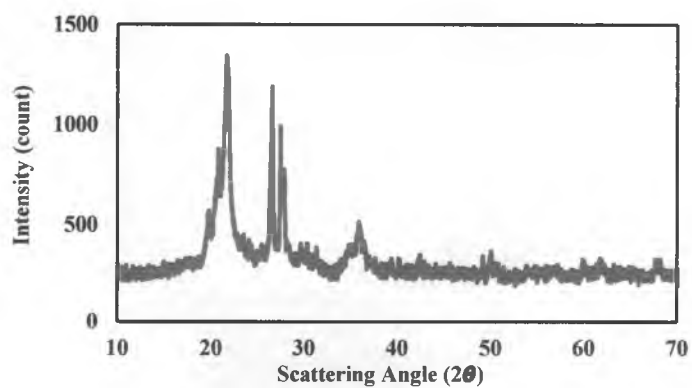


G. XRD signals of opal-CT siliceous mudstone in the Monterey area

1. Sample 11.1, Whispering Pines Park

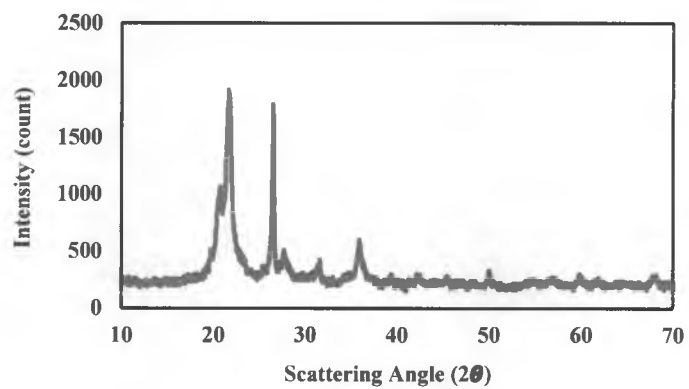


2. Sample 11.5, Whispering Pines Park

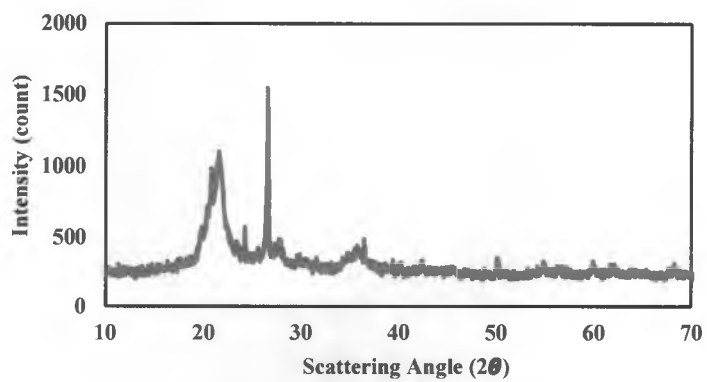


H. XRD signals of opal-CT porcelanite samples in the Monterey area

1. Sample 6.1, Pacific Meadows Park

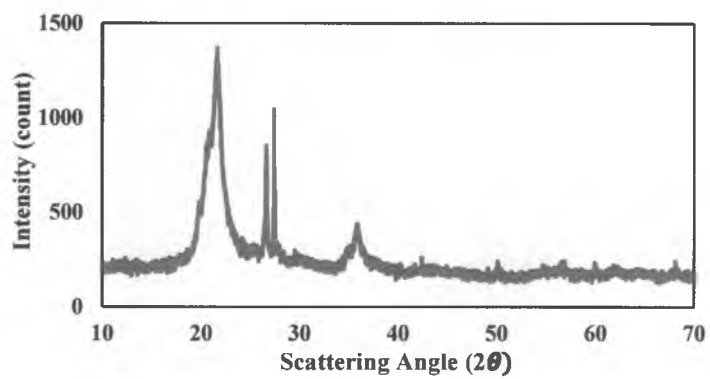


2. Sample 15.4, Saddle Road

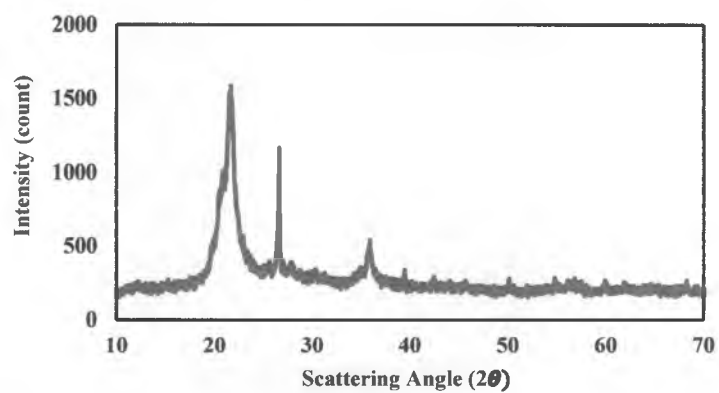


I. XRD signal of opal- CT diatomaceous porcelanite samples in the Monterey area

1. Sample 3.2, Laureles Grade

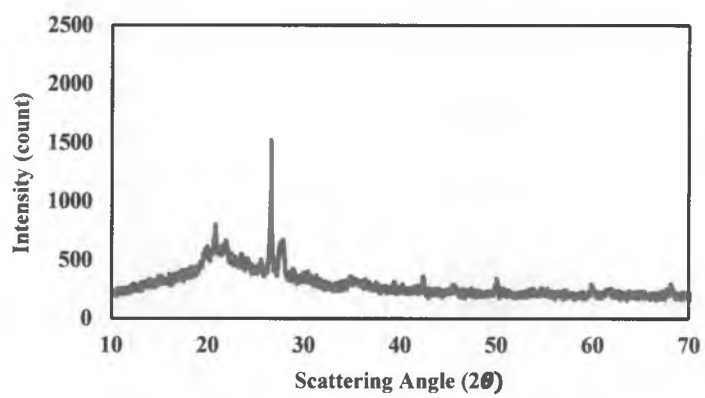


2. Sample 4.1, Laureles Grade



J. XRD signal of opal-A to opal-CT diatomite sample in the Monterey area

1. Sample 1.1, Toro Road



K. XRD signals of highly detritus diatomite sample in the Monterey area

1. Sample 16.2 Toro Road

